AD-A178 979 DEVELOPMENT OF A GENERALIZED MODEL FOR A THREE COMPONENT PLASMA(U) AIR FORCE INST OF TECH WRIGHT-PATTERSON AFB OH SCHOOL OF ENGINEERING 1/1

UNCLASSIFIED J C LUCAS JAN 87 AFIT/GNE/EN/87M-4 F/G 20/9 NL

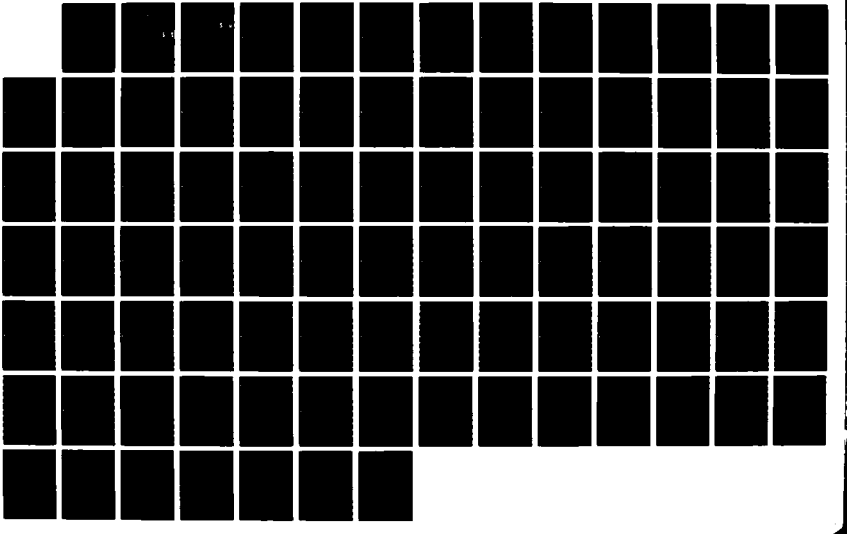

MIC

DEVELOPMENT OF A GENERALIZED MODEL FOR A THREE COMPONENT PLASMA

THESIS

John C. Lucas
First Lieutenant, USAF

AFIT/GNE/87M-4

DEPARTMENT OF THE AIR FORCE
AIR UNIVERSITY
AIR FORCE INSTITUTE OF TECHNOLOGY

Wright-Patterson Air Force Base, Ohio

AFIT/GNE/87M-4

DEVELOPMENT OF A GENERALIZED MODEL FOR A THREE COMPONENT PLASMA

THESIS

John C. Lucas
First Lieutenant, USAF

AFIT/GNE/87M-4

AFIT/GNE/EN/87M-4

DEVELOPMENT OF A GENERALIZED MODEL FOR A THREE COMPONENT PLASMA

THESIS

Presented to the Faculty of the School of Engineering

of the Air Force Institute of Technology

Air University

In Partial Fulfillment of the

Requirements for the Degree of

Master of Science in Nuclear Science

John C. Lucas, B.S.

First Lieutenant, USAF

January 1987

Approved for public release; distribution unlimited

Acknowledgements

Many thanks to my advisor Dr. William Bailey, for his invaluable assistance.

CONTENTS

List of Figures

ABSTRACT

The purpose of this study is to develop a generalized model of a three component plasma which predicts the density profiles of the charged particles. The plasma was modeled using a finite difference solution to the charged particle continuity and momentum equations. The plasma-sheath boundary is treated by applying the Bohm criterion.

The code developed was sucessful in modeling simple one component diffusion. However attempts to apply the model to two component plasmas resulted in numerical instabilities and therefore prevented application of the model to a three component plasma. Though the exact cause of these instabilities were not determined during the course of the research; facts point to flaws in the positive ion drift velocity calculation and wall flux boundary condition.

I. Introduction

Background

Research on efficient negative ion sources for particle beam weapons and advances in plasma processing of semiconductor materials have stimulated new interest in the investigation of discharges in electronegative gases. Of particular interest to the Air Force is development of high current density, low emittance ion sources. However before these plasmas can be effectively used as negative ion sources, the spatial profile of the negative ions in relation to the other charged particles must be known. A knowledge of the spatial profiles will not only make it possible to efficiently extract negative ions from the plasma, but also allow the optimization of design parameters, such as gas pressure and temperature.

Radio-frequency gas discharges are currently used to etch submircometer circuits in semiconductors (7:77). Energetic ions that impinge on the semiconductor material deliver an activation energy to the surface of the semiconductor (7:77), thereby etching the material. The quality of the etch is dependent on the character of the plasma sheath, and the type and density of ions in the plasma (7:77). In order that reliability and consistency be obtained in plasma processing, a detailed knowledge of the spatial profiles and plasma processes (ion generation/loss, particle fluxes, etc.) is required (12:103).

Though we have a definite need to fully understand the processes in plasmas, our current knowledge is incomplete (6:145). The study of discharges in gases began as early as 1924 with the work of Schottky and Langmuir (2:1). This early work concerned discharges in two component plasmas, i.e., plasmas comprised of electrons and positive ions. Schottky's treatment describes the motion of charged particles in the plasma by assuming the particle fluxes result form a balance between a diffusive (density gradient) flux and a electric field driven flux. The predictions made by Schottky's theory agree well with observations (8:4699) Several attempts have been made to calculate the spatial profiles in three component plasmas (see References 3,8,16). Many of these attempts (e.g. Reference 8) are extensions of Schottky's theory to three component plasmas (3:376). However, the results of these extensions and other attempts are contradictory or of limited applicability.

Problem and Scope

The purpose of this study is to develop a generalized model of a three component plasma which predicts spatial density profiles of the charged particles. Throughout this report the term model refers both to the computational method employed and the relevant plasma kinetic processes included.

Approach

The planned approach of this research was threefold. The first step was to review current theoretical efforts on the determination of the spatial variations of the charged species in low and medium pressure gas discharges. This review would form a basis for determining the plasma processes which must be considered (modeled) and also guide the development of a computational method. A further benefit of the review is that it will provide sources for comparison with theory and experiment leading to model validation. The second step was to develop a model and validate it for plasmas consisting of electrons and positive ions only. This initial model was to be developed in slab geometry (one dimensional) and later cast into cylindrical geometry. With the model validated for the two component plasma the last step would be to validate the model for a three component plasma.

II. Plasma Theory

In this chapter we shall look at the general motion of charged particles in two and three component plasmas. We will also look at the equations which govern this motion and the relevant production and loss processes which occur in a plasma. We shall begin by looking at the general physics of a plasma. To do this we will first consider a plasma consisting of only electrons and positive ions. After this we will expand the discussion to a three component plasma.

The electrons in a plasma, because they are more mobile (i.e. because of their smaller mass and higher temperature, they have a larger velocity), will initially diffuse to the walls of a discharge tube (where recombination occurs) faster than the ions (positive ions in this case). Therefore the electrons in the plasma are lost at a greater rate than the positive ions. This causes a charge imbalance to occur in the plasma, which in turn creates an electric field. The field that develops acts to reduce the flux of the electrons and increase that of the ions. This field increases until the electron and ion fluxes are equal. When this occurs, the self-consistant charge imbalance does not change in time and a quasi-stationary state (4:197) is achieved. This situation is called ambipolar diffusion.

The presence of negative ions in the plasma complicates the diffusion process. As in the two component case, the electrons will be initially lost at a greater rate than the

ions (both positive and negative). However, the presence of the negative ions will affect the net space charge and thus the electric field. The change in the electric field will in turn affect the density profiles and fluxes of the charged particles.

The effect the presence of the negative ions have on particle diffusion is critically dependent on the detachment rate (15:1377). If the detachment rate is small, so that the dominant loss of negative ions is recombination on the wall, the flux of all three species is directed to the wall. If, on the other hand, the dominant loss of negative ions is due to detachment, the negative ions have very little effect on the diffusion of the electrons. In this case the diffusion and density profiles resemble that of the ambipolar case (15:1377).

Loss and Production Processes

In this study we shall limit the production and loss processes in the plasma to four processes. The first three processes, ionization, (z), dissociative attachment, (σ), and electron impact detachment, (d), occur throughout the discharge volume. Writing the processes symbolically:

Ionization (z)	$e + A \text{ --- } A^+ + 2e$
Attachment (σ)	$e + A \text{ --- } A^-$
Detachment (d)	$A^- + e \text{ --- } A + 2e$

Note that in defining the ionization and attachment rates we have included the background gas (neutral particle) density in the expressions z and α ; that is, $z = N\langle\sigma v\rangle$, where N is the neutral particle density and $\langle\sigma v\rangle$ is the reaction cross section for ionizing collisions between electrons and neutrals. Similarly, $\alpha = N\langle\sigma v\rangle$, where $\langle\sigma v\rangle$ is the reaction cross section for attachment.

The fourth process is recombination at the discharge tube wall. These four processes are summarized in Table 1.

PROCESS	Electron	+ Ion	- Ion
Ionization	Gain	Gain	-
Attachment	Loss	-	Gain
Detachment	Gain	-	Loss
Recombination at Wall	Loss	Loss	Loss

TABLE 1. Summary of Plasma Production and Loss Processes

Writing the volume processes in equation form gives:

$$(\partial n_e/\partial t)_c = (z-\alpha)n_e + dn_e n_- \quad (1)$$

$$(\partial n_-/\partial t)_c = \alpha n_e - dn_e n_- \quad (2)$$

$$(\partial n_+/\partial t)_c = z n_e \quad (3)$$

where n_e is the electron density;

n_- is the negative ion density;

n_+ is the positive ion density.

These equations represent the local time rate of change of charged particle density due to collisions (as denoted by the subscript c).

Plasma Equations

The transport of charged particles in a plasma is governed by the Boltzmann equation (1:206)

$$\partial f/\partial t + \underline{v} \nabla f + (\underline{F}/m)\, \partial f/\partial \underline{v} = (\partial f/\partial t)_c \qquad (4)$$

where $f(\underline{x},\underline{v},t)$ is the particle distribution function. If we assume that no external forces act upon the plasma, the expression for the force ($\underline{F}$) can be written as $\underline{F}=q\underline{E}$, where $\underline{E}$ is the electric field generated by the net space charge and q is the charge on the particle (e.g. q=-e for an electron). Substituting this into equation (4) gives:

$$\partial f/\partial t + \underline{v} \nabla f + (q\underline{E}/m)\partial f/\partial \underline{v} = (\partial f/\partial t)_c \qquad (5)$$

Taking the zeroth moment of equation (5) yields the continuity equation (5:156):

$$\partial n/\partial t + \nabla\, n\langle \underline{v} \rangle = S_{coll} \qquad (6)$$

where $S_{coll}=(\partial n/\partial t)_c$ and $\langle \underline{v} \rangle$ is the average velocity of the particle. S_{coll}, therefore is the density change due to collisions, i.e. equations (1)-(3). Substituting S_{coll} for

each of the three species yields the three continuity equations:

$$\partial n_\varepsilon/\partial t = (z-\sigma)n_\varepsilon + dn_\varepsilon n_- - \nabla \cdot \Gamma_\varepsilon \quad (7)$$

$$\partial n_+/\partial t = zn_\varepsilon - \nabla \cdot \Gamma_+ \quad (8)$$

$$\partial n_-/\partial t = \sigma n_\varepsilon - dn_\varepsilon n_- - \nabla \cdot \Gamma_- \quad (9)$$

where Γ_S is flux of species "S".

The first moment of equation (5) gives the momentum equation (5:162):

$$mn\partial\langle \underline{v}\rangle/\partial t + mn(\langle \underline{v}\rangle \cdot \nabla)\langle \underline{v}\rangle + kT\nabla n - q\underline{E}n = mn\nu_{MT}(\langle \underline{v}^N\rangle - \langle \underline{v}\rangle) - m\langle v\rangle S_{COLL} \quad (10)$$

where:

ν_{MT} is the momentum transfer frequency (collisions with neutrals);

$\langle \underline{v}^N\rangle$ is the average velocity of neutrals, which is assumed to be zero (the neutral particle velocity is assumed Maxwellian);

k is the Boltzmann constant and T is the species temperature. In deriving this expression for the momentum equation, it is assumed that the pressure tensor can be represented as a scalar pressure ($kT\nabla n$).

Equations (7)-(9) and (10) form the basic equations needed to model plasma behavior. These equations are then complemented with Poisson's equation:

$$\nabla \underline{E} = (e/\varepsilon_o)(n_+ - n_E - n_-) \qquad (11)$$

III. Review of Plasma Models

Several attempts to model plasma behavior have been made. In this section we shall review four models in an attempt to identify critical assumptions and demonstrate the limitations and the disparity in the results of these approaches. The four models which shall be reviewed are: (1) Ambipolar; (2) Self and Ewald; (3) Lee and Lewis; (4) Von Engel and Edgley.

Ambipolar Model

The ambipolar model is the simplest of the models. In this model it is assumed that the plasma has reached a steady state; therefore, the time dependence of the continuity and momentum equations is eliminated. The momentum equation for the electrons becomes (in one dimension):

$$n_\varepsilon m\langle v\rangle \partial\langle v\rangle/\partial x + kT_\varepsilon \partial n_\varepsilon/\partial x - n_\varepsilon qE = -mn_\varepsilon \nu_{MT} \langle v\rangle \qquad (12)$$

Substituting for the particle charge (q=-e) and assuming that the inertial term ($\langle v\rangle \partial\langle v\rangle/\partial x$) can be ignored due to the small mass of the electron:

$$kT_\varepsilon \partial n_\varepsilon/\partial x + n_\varepsilon eE = -mn_\varepsilon \nu_{MT} \langle v\rangle \qquad (13)$$

This equation can be used to solve for the ambipolar drift velocity, $\langle v \rangle$. To do this we first define mobility as $\mu = |q|/m\nu$ (1:137). We will also define a diffusion coefficient using the Einstein relation, $D = kT/m\nu$ (1:137). Using these definitions in equation (13), one obtains:

$$\langle v \rangle = -(D_\varepsilon/n_\varepsilon)\partial n_\varepsilon/\partial x - \mu_\varepsilon E$$

But flux, Γ_ε is equal to $n_\varepsilon \langle v \rangle$, therefore:

$$\Gamma_\varepsilon = -D_\varepsilon \partial n_\varepsilon/\partial x - \mu_\varepsilon E n_\varepsilon \qquad (14)$$

Assuming the positive ion flux can be written in the same fashion, we have:

$$\Gamma_+ = -D_+ \partial n_+/\partial x - \mu_+ E n_+ \qquad (15)$$

It is next assumed that the charged particle density profiles are approximately the same; therefore, $n_e = n_+ = n$ (1:137). In the steady state, the electron and ion fluxes are equal. Therefore, by setting equations (14) and (15) equal to each other and assuming quasi-neutrality ($n_e = n_+ = n$) it is possible to derive an expression for the electric field. The resulting expression (1:138):

$$E = \{(D_+ - D_\varepsilon)/(\mu_+ + \mu_\varepsilon)\} \nabla n/n \qquad (16)$$

Substituting equation (16) into equation (14) results in (1:138):

$$\Gamma = -D_A \partial n/\partial x \qquad (17)$$

where D_A is the ambipolar diffusion coefficient; $D_A=(\mu_+ D_- + \mu_- D_+)/(\mu_+ + \mu_-)$.

Substitution of equation (17) into equation (7), (noting that $\partial n/\partial t = 0$ in steady state), we obtain (α and d are zero for a two component plasma):

$$D_A \partial^2 n/\partial x^2 + zn = 0 \qquad (18)$$

Boundary conditions must be established before this differential equation can be solved. We expect that the discharge is symmetric about the center of the discharge tube (two parallel plates separated by a distance 2L in our case); therefore the flux a the center (x=0) should be zero. If the flux is zero at the center of the discharge, then by equation (17) $(\partial n/\partial x)_{x=0}=0$. Ignoring the development of a sheath area, it is assumed that the particle density at the discharge wall (x=L) is zero. Applying these boundary conditions, equation (18) is easily solved to obtain (for rectangular 1-D):

$$n = n_{e0}\mathrm{Cos}(\pi x/2L) \qquad (19)$$

where $[z/D_A]^{1/2}=\pi/2L$.

Substituting equation (19) into equation (16) gives:

$$E = ((D_+ - D_E)/(\mu_+ + \mu_E))(2L/\pi)\mathrm{Tan}(\pi x/2L) \qquad (20)$$

An example of the ambipolar density profile is given in Figure 1. Though in our development we assumed the particle profiles to be the same, the figure illustrates the difference in the two profiles which must exist to develop the field given by equation (20).

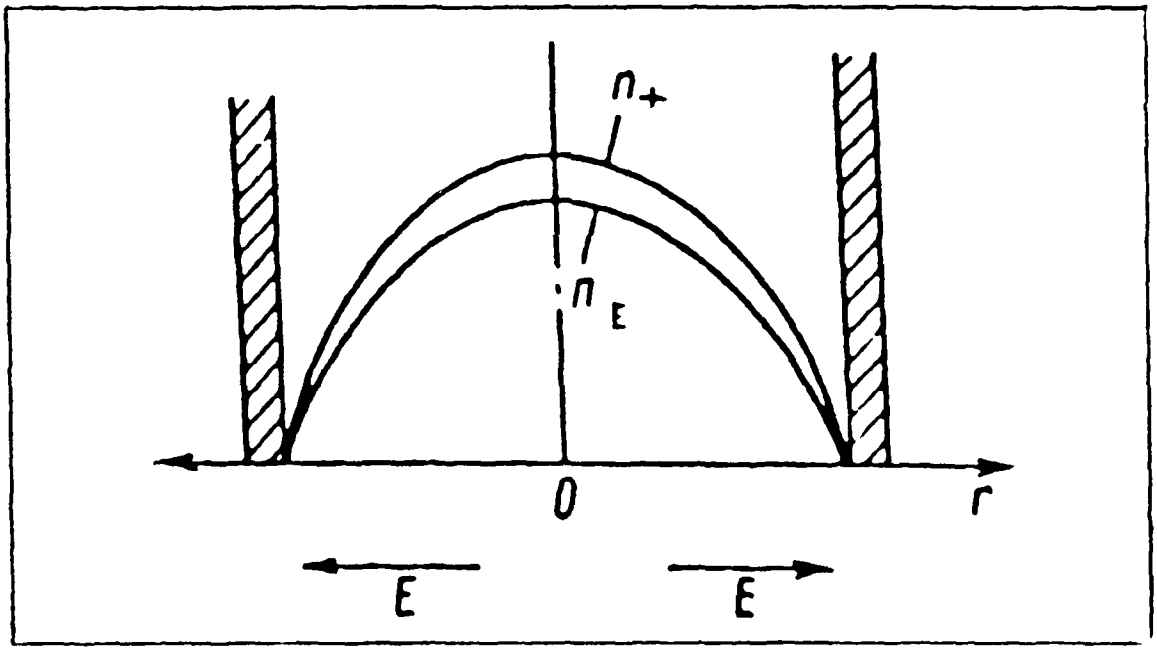

Figure 1 Charged Particle Profiles Under Ambipolar Conditions (Golant:198)

Self and Ewald

Like the ambipolar model, Self and Ewald is an analytic solution of a two component plasma. It will be instructive to first look at the main differences between this model and

the ambipolar model.

The first difference between this model and the ambipolar model can be seen in the momentum equations. Self and Ewald make the same assumptions in developing their electron momentum equation as are made in the ambipolar model, but unlike the ambipolar model, they do not assume the electron equation can also be applied to the positive ions. In their development, Self and Ewald retain the inertial term ($\langle v \rangle \partial \langle v \rangle / \partial x$) in the ion momentum equation.

An additional important difference in Self and Ewald's model is that they do not assume a zero density at the discharge wall. They instead attempt to model the plasma-sheath boundary by applying the Bohm criterion (14:2487).

With the major differences in this model and the ambipolar model identified, an outline of Self and Ewald's model can be discussed (a detailed development of Self and Ewald's model is included as Appendix A). Like the Ambipolar model, Self and Ewald assume quasi-neutrality ($n_e = n_+ = n$). This reduces the problem to one of solving three equations, a continuity equation and two momentum equations. Normalization of the continuity and momentum equations results in equations (A-12)-(A-14) (in one dimension).

$$d(su)/ds + u\,d[Ln(n)]/ds = A \qquad \text{(A-12)}$$

$$u = R'(d\Gamma/ds) - d[Ln(n)]/ds \qquad \text{(A-13)}$$

$$u + u(du/ds) = d\Gamma/ds - \tau\, d[Ln(n)]/ds \qquad \text{(A-14)}$$

where:

A is the ratio of the ionization rate to the sum of the momentum transfer collision frequency and ionization rate;

u is the normalized particle velocity;

s is the normalized spatial coordinate;

η is the normalized electric potential;

τ is ratio of the ion temperature to the electron temperature;

R' is a normalizing factor ($m_+\nu_+/m_E\nu_E$).

Making the normalized particle velocity the independent variable, Self and Ewald solve for ds/du, s, $Ln(n/n_0)$, and the normalized potential (η) (n_0 is the particle density at x=0). The resulting equations are:

$$ds/du = \{(1+\tau)-u^2\}/[A(1+\tau)+ R^{"}u^2] \qquad (A\text{-}20)$$

$$s=[(1+\tau)^{1/2}(R^{"}+A)]/[A^{1/2}(R^{"})^{3/2}]Tan^{-1}(Wu)- u/R^{"} \qquad (A\text{-}21)$$

$$Ln(n/n_0) = -\{[R^{"}+A]/(2R^{"})\}Ln(Y) \qquad (A\text{-}22)$$

$$\eta = -\{(1-\tau/R')(R^{"}+ A)/[2(R^{"})^2]\}Ln(Y)-u^2/[2(1+R')] \qquad (A\text{-}23)$$

Where

$R^{"}= (1+1/R')$;

$W = [(1+1/R')/A(1+\tau))^{1/2}]$;

$Y = \{(R^{"}+A]u^2+A(1+\tau)\}/[A(1+\tau)]$.

Equation (A-20) is used to place an upper bound on the variable u. The upper limit of u, is the value which makes equation (A-20) equal to zero. When this condition is

reached, the ion velocity is equal to the ion sound speed (the Bohm criterion) (14:2487). The discharge boundary is the value of "s" when the upper value of u is substituted into equation (A-21) (14:2488). Therefore in this model the density is not constrained, as it was in the ambipolar model (i.e., the density made to be zero at the discharge boundary).

The density profile at the discharge boundary is dependent on the pressure of the background gas. Self and Ewald incorporate this pressure dependence in their equations by use of the pressure parameter (A) (14:2488). In low pressure plasmas the ionization rate is much greater than the ion collision frequency (14:2487) (mean free path between collisions is large); therefore, A approaches unity. In these cases the density profiles approach that of the Free-Fall theory (14:2488). Free-Fall theory assumes that that the motion of the charged species is not impeded by collisions. The velocity of the particles in this theory is equal to that the particles would have by falling through the electric potential existing in the plasma. As A approaches zero (high pressure plasmas) the density profile transitions to the results of the ambipolar model (14:2488). Figure 2 depicts this transition from the free fall theory to the ambipolar results for increasing A.

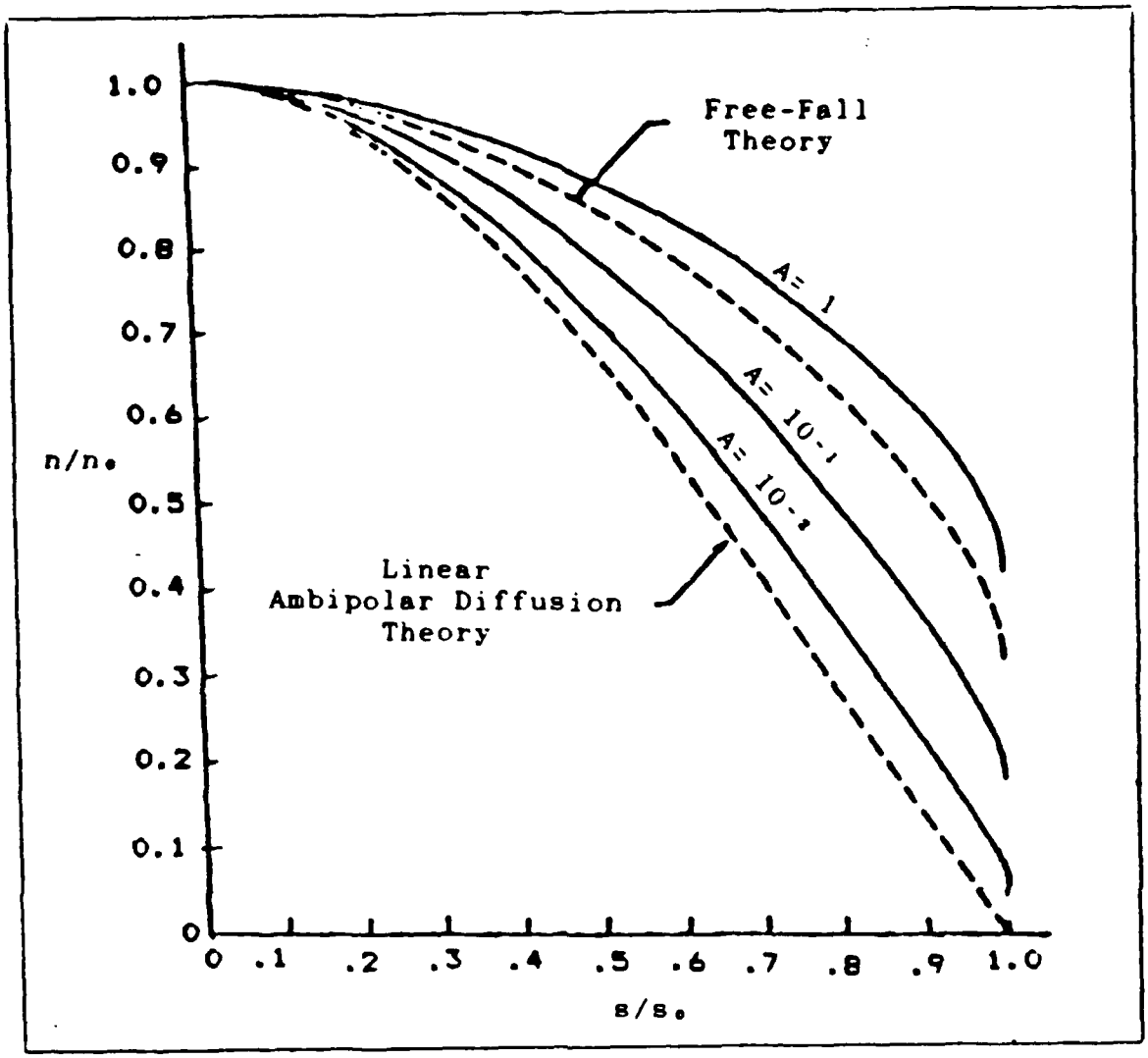

Figure 2 Density Profiles for Plane-Symmetric Discharge (Self:2488)

Lee and Lewis

Lee and Lewis' model was originally developed for discharges in oxygen; however, given the ionization, attachment, and detachment rates for a particular gas, the model can be applied. A detailed analysis of this model was made in reference 2.

We will first examine the assumptions Lee uses to develop his solution. As before, we shall begin with the

continuity and momentum equations. Lee assumes steady state solutions; therefore, the continuity equations (7)-(9) reduce to (in cylindrical geometry):

$$r^{-1}\partial(r\Gamma_E)/\partial r - (z-\alpha)n_E - dn_E n_- = 0 \quad (21)$$

$$r^{-1}\partial(r\Gamma_+)/\partial r - zn_E = 0 \quad (22)$$

$$r^{-1}\partial(r\Gamma_-)/\partial r - \alpha n_E + dn_E n_- = 0 \quad (23)$$

where r is the radial coordinate in cylindrical geometry.

As in the ambipolar model, Lee assumes the fluxes of each species can be written as:

$$\Gamma_E = -D_E n_E/r - \mu_E n_E E \quad (24)$$

$$\Gamma_+ = -D_+ n_+/r + \mu_+ n_+ E \quad (25)$$

$$\Gamma_- = -D_- n_-/r - \mu_- n_- E \quad (26)$$

Using that in the steady state, $\Gamma_+ = \Gamma_E + \Gamma_-$ and Poisson's equation, Lee is able to eliminate the electric field from these equations. The end result is a set of four differential equations for the electron and negative ion fluxes and densities.

$$x^{-1}(xy_3)' = [(z-\alpha)/\alpha]y_1 + (d/\alpha)y_2 \quad (27)$$

$$x^{-1}(xy_4)' = y_1 - (d/\alpha)y_2 \quad (28)$$

$$y_1' + 2(T_-/T_E)y_2' = -Ay_3 - By_4 \quad (29)$$

$$y_1'y_2 - (T_-/T_E)y_2'y_1 = (B-A)y_1y_4 - Cy_2y_3 \quad (30)$$

where

x is the normalized radius (r/R) (R is outer tube radius)

y_1 is the normalized electron density $[n_\varepsilon(r)/n_\varepsilon(0)]$

y_2 is the normalized negative ion density $[n_-(r)/n_\varepsilon(0)]$

y_3 is a normalized electron flux $[\Gamma_\varepsilon(r)/\alpha n_\varepsilon(0)R]$

y_4 is a normalized negative ion flux $[\Gamma_-(r)/\alpha n_\varepsilon(0)R]$

$A = m_+\nu_+\alpha R^2/T_\varepsilon$; $B=A+(m_-\nu_-\alpha R^2/T_\varepsilon)$; $C= m_\varepsilon\ _\varepsilon\alpha R^2/T_\varepsilon$

This set of four differential equations (eq. (27)-(30)) is solved using a fourth order Runge-Kutta method (2:24).

Like the ambipolar model, Lee ignored the sheath region and assumed the density of all three species to be zero at the wall. Lee's second boundary condition was that the particles fluxes at the axis were zero because of symmetry.

In testing this model the primary problem was the sensitivity of the calculation and subsequent convergence to the selected value of the on-axis ratio of negative ions to electrons (h). This parameter was the starting value used in the numerical integration. The convergence to a solution was slow for a poor choice of h. This sensitivity to the parameter h is discussed in detail in reference 2.

An example of the electron and negative ion profiles predicted by Lee's model is shown in Figure 3. The profiles in Figure 3 are representative of the profiles presented in Lee's paper (Ref. 8) and Clouse's analysis (Ref. 2). In particular we should note from figure 3 that Lee's code predicts that the negative ions are distributed throughout

Von Engel and Edgley

This model resembles Lee's model in many ways. As before we shall proceed by discussing the development of the continuity and momentum equations, and then discuss the boundary conditions applied in the model.

The particle continuity equation and the electron momentum equation used by Von Engel are the same as those used by Lee. The ion momentum equations however differ significantly. In developing his positive ion equation Von Engel assumes that the electric field driven drift velocity will be much greater than the positive ions' thermal velocity; therefore, the term involving the ion temperature can be ignored. Making this assumption leaves us with the following (in cylindrical geometry):

$$n_+ \partial\langle v_+\rangle/\partial r = -eE/(m_+\langle v_+\rangle) - \nu_+ - z n_\Sigma \qquad (31)$$

For the negative ions Von Engel assumes that the negative ion velocity will be primarily thermal. He further assumes the the motion of the negative ions will be governed by "the balance between of the outward diffusion due to the density gradient and the inward drift due to the electric field" (3:378). Using these assumptions, Von Engel drops the inertial term from the negative ion momentum equation. This reduces the negative ion momentum equation to:

$$\partial n_-/\partial r = e n_- E/(kT_-) - [\nu_- m_-/(kT_-)] n_- \langle v_-\rangle \qquad (32)$$

Like Lee, Von Engel uses the continuity equations, momentum equations, and Poisson's Law to develop a set of differential equations which he solves using a fourth order Runge-Kutta method.

The other difference between Lee's and Von Engel models is the boundary condition at the wall. Where Lee assumes a zero density, Von Engel assumes a condition much like that of Self and Ewald's model. Von Engel terminates his numerical integration at the position where the following boundary condition for the electrons is met (3:379):

$$u_E = \langle v_E \rangle / v_{ss} = (2m_+/\pi m_E)^{1/2}$$

With this boundary condition Von Engel assumes that the discharge boundary is the point where the normalized electron velocity, u_E, is equal to the ratio of the electron thermal velocity to the ion sound speed (3:379). In this way, Von Engel is able to place a boundary condition on the electrons without constraining the density. Von Engel believes that forcing all particles densities to be zero at the wall over constrains the solution (3:376).

Von Engel noted computational problems similar to Lee's in that the process is slow and sensitive to the choice of h (3:381). An example of Von Engel's results are presented in figure 4.

normalizaton, Lee used n_-/n_{-0} (where n_{-0} is the negative ion density on axis) while Von Engel used n_{e-}/n_{e0}. The most striking difference in the two author's profiles is that Von Engel predicts that the negative ions are confined near the center of the discharge, while Lee's negative ions are distributed throughout. In Figure 5 we have attempted to demonstrate this difference by placing Von Engel's negative ion profile on Lee's plot (Figure 3). This difference may be related to a difference in detachment rate (as reported by Tsendin). Unfortunately this could not be determined from the information given in the authors' papers.

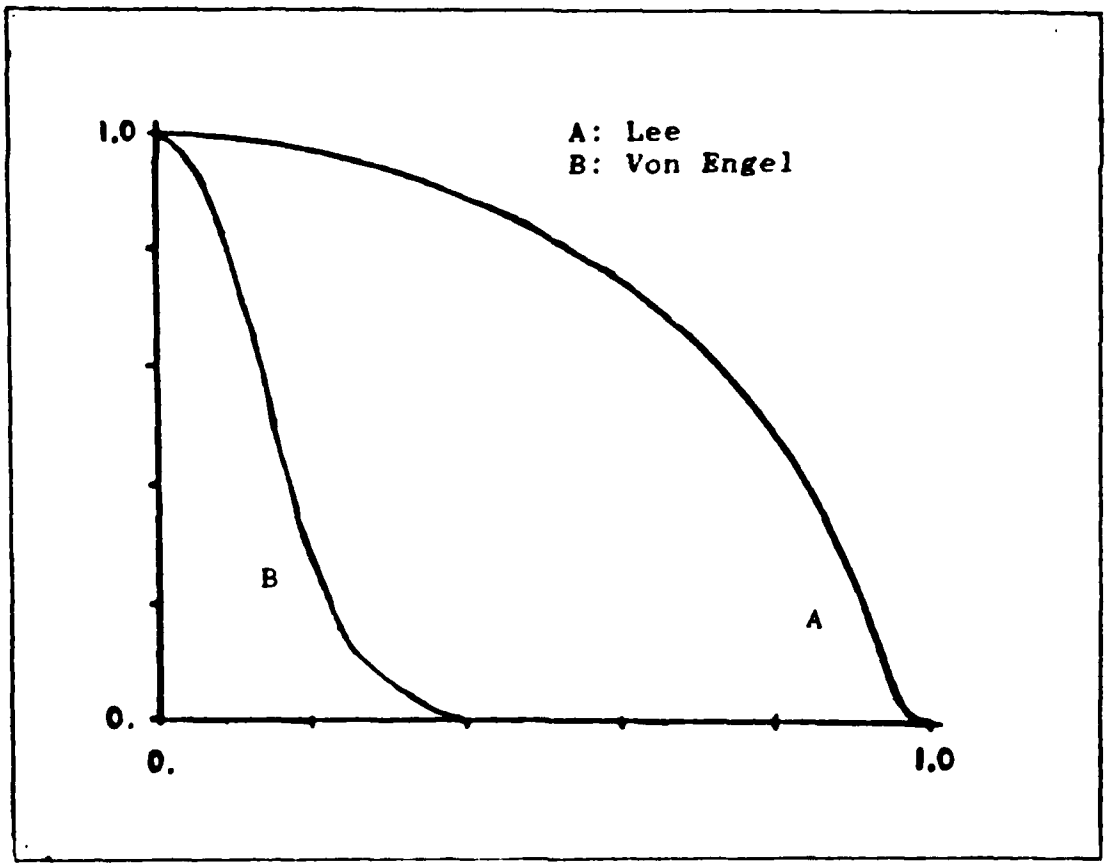

Figure 5 Comparison of Lee's and Von Engels Negative Ion Profiles (Adapted Lee:4703)

IV. Model Development

The numerical method employed is based on a finite difference solution of continuity and momentum equations of the three charged species. One advantage of this method is that it would allow a time development of the density profiles and electric field. This removes the sensitivity of the solution from the choice of initial conditions (which was seen in the solutions of Lee and Von Engel). Because the density profiles are allowed to adjust themselves in time, our initial profiles can evolve into the steady state solution, as opposed to requiring an iterative selection of new initial conditions when the solution does not meet the boundary conditions in the steady state (as in Lee and Von Engel's solutions).

The discussion in this chapter is divided into three parts. The first of these describes the general finite differencing method (as applied to a flux divergent problem). The second part will cover the development of the finite differenced plasma equations (continuity and momentum). The discussion in this chapter ends with a general description of the model code.

Finite Differencing Method

To explain the finite differencing method, the discussion below will be limited to slab geometry (in particular the discharge between two parallel plates);

however the general principles are the same for all geometries. As in any finite differencing scheme, space is divided into cells. In this case, "space" is the discharge area between one wall of the discharge tube and the center (because the discharge is symmetric about the center only one side of the discharge need be modeled).

To explain the setup of the finite differencing grid and general principle of the finite differencing method, we shall consider a simple one-dimensional flux divergent problem. For this example, assume that "space" is divided into five cells (see Figure 6). Each cell (i), has a density n_i, defined at the cell center. Fluxes are defined at the cell boundaries.

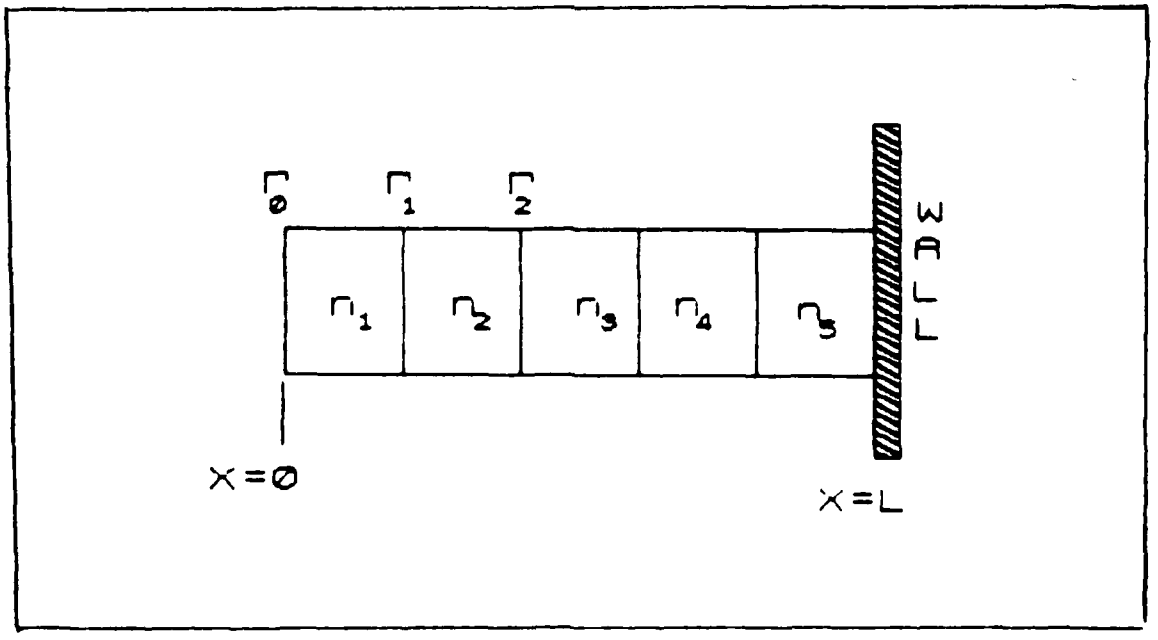

Figure 6. Example of Finite Difference Grid for Flux Divergent Problem

Looking now at a single cell, we find that the change in the number of particles in unit time is given by:

{change in density/unit time}dVol = {Net Flux into Cell}dA + {Production/Losses}dVol

In this example, we shall assume that there are no production or loss mechanisms within the volume of the cell; therefore, the change in the number of particles in a cell will be determined by the fluxes into and out of the cell. Putting our conservation statement into equation form:

$$(\Delta n/\Delta t)\Delta x\Delta y\Delta z = -(\Gamma_{out} - \Gamma_{in})\Delta y\Delta z$$

This is actually the continuity equation (eq. 6) with the collisional production (S_{COLL}) term equal to zero; therefore:

$$\partial n/\partial t = -(\Gamma_{out} - \Gamma_{in})/dx$$

Approximating the time derivative with a forward difference gives:

$$(n(t+\tau) - n(t))/\tau = -(\Gamma_{out} - \Gamma_{in})/dx \qquad (33)$$

where τ is the time step interval. From Figure 6 we see that for the first cell, the "in flux" is Γ_0 and the "out

flux" is Γ_i . Letting h=dx and using an index i to denote cell numbers, equation (33) becomes:

$$[n_i(t+\tau) - n_i(t)]/\tau = -(\Gamma_i - \Gamma_{i-1})/h \qquad (34)$$

Equation (34) can be solved for $n_i(t+\tau)$ to give:

$$n_i^{j+1} = n_i^j - (\tau/h)(\Gamma^j - \Gamma^j) \qquad (35)$$

where j denotes the current time step (t) and j+1 denotes the next time step (t+τ).

So far in our discussion we have assumed that the finite difference equations (e.g., equation (35)) are numerically stable. This will only be true if the Courant condition is met. The Courant condition is (10:626):

$$|v_c|\tau/h \leq 1 \qquad (36)$$

where v_c is the characteristic speed at which information travels through the finite difference grid. In the example above, the characteristic speed is the maximum velocity of the particles. The necessity of obeying the Courant condition can be better understood at examining the way in which the density of a cell is calculated. The cell density is, in part, calculated from information (fluxes) gained from the boundaries of that cell. If the time step (τ) is to large (i.e., $v_c\tau > h$), the information (the fluxes in

our case) required by the differencing scheme lies at points outside the boundaries of the cell. Since the fluxes will not be defined at these points, a lack of information exists. This lack of information gives rise to an instability (10:627). Therefore, provided that $(\tau/h) \leq (1/v_c)$, the Courant condition assures us that our finite differencing scheme will remain numerically stable.

We now increase the complexity of our example by including the influence of an electric field. In this way, we can examine the use of the finite differencing scheme to calculate plasma parameters (in a simple plasma). For this example we shall assume ambipolar conditions; therefore, the electron continuity equation and flux are given by:

$$\partial n/\partial t = -(\partial \Gamma/\partial x) + zn \tag{37}$$

$$\Gamma = -D\partial n/\partial x - \mu_E E \nabla n \tag{38}$$

(For the purpose of this example only the development of the electron equations will be discussed). Finite differencing of equations (37) and (38) results in the following:

$$n_i^{j+1} = n_i^j - (\tau/h)(\Gamma_i^j - \Gamma_{i-1}^j) + z\tau n_i^j \tag{39}$$

$$\Gamma_i^j = -(D_E/h)(n_{i+1}^j - n_i^j) - (\mu_E E_i^j/2)(n_{i+1}^j + n_i^j) \tag{40}$$

Before proceeding, a few notes on equation (40) are in order. The fluxes in the finite differencing grid are calculated on the cell boundaries; therefore, we shall

calculate the density and gradient terms in equation (40) at the cell boundaries. Because the densities are defined at the cell centers, the density at the cell boundary is approximated by averaging the densities of the cells adjacent to the boundary (thus giving the $[n_i+n_{i+1}]/2$ term).

Before equations (39) and (40) can be developed into a set of equations which can be used to calculate the cell densities, boundary conditions must be established. For this example, it will be convenient to establish boundary conditions on the flux at the discharge axis (x = 0) and the discharge wall (x = L). Assuming that the discharge will be symmetric about the discharge axis, the flux at x=0 is zero (i.e. $\Gamma_E = 0$). For the wall condition we shall assume the flux at the wall is equal to a constant (i.e. $\Gamma_E = L$).

Substituting the flux expression (40) into (39) results in an expression which can be used to solve for the electron density in cells 2 thru N-1,as shown below:

$$n_i^{j+1} = n_i^j - \tau\{(D_E/h^2)(n_{i-1}^j - 2n_i^j + n_{i+1}^j) - (\mu_E/2)[(n_{i+1}^j + n_i^j)E_i^j - (n_i^j - n_{i-1}^j)E_{i-1}^j]\} + z\tau n_i^j \qquad 2 \le i \le N-1 \qquad (41a)$$

Incorporating the boundary conditions for Γ_1 and Γ_N in equation (39), yields:

$$n_1^{j+1} = n_1^j - \tau\{(D_E/h^2)(n_{i+1}^j - n_i^j)/h - (\mu E_i^j/2)(n_{i+1}^j + n_i^j)\} + \tau z n_i^j \qquad i=1 \qquad (41b)$$

$$n_N^{j+1} = n_N^j - \tau\{ L - (D_E/h^2)(n_N^j - n_{N-1}^j) - (\mu_E E_{N-1}^j/2)(n_N^j + n_{N-1}^j)\} + \tau z n_N^j$$

$$i=N \qquad (41c)$$

A similar set of equations can be developed for the positive ions.

The electric field is calculated using Gauss' Law.

$$\{E(x) - E(0)\} = (e/\varepsilon_0) \int_C^X (n_+ - n_E)\, dx'$$

Approximating this integral with a summation, the electric field, directed toward the boundary is:

$$E_i = \sum_{r=1}^{N} (n_{+,r} - n_{E,r})h$$

where dx has been replaced by h and due to symmetry, $E_0=0$.

Summarizing the procedure used in calculating the density profiles:

1) Start with a set of initial conditions for the electric field and electron and positive ion densities.

2) Calculate the electron and ion densities at an advanced time using the density equations.

3) Compute the electric field in this advanced time using the new densities.

4) Increment time (i.e. redefine j+1 values as j values), repeat until process converges.

Once again the Courant condition (equation (36)) must be obeyed for the differencing scheme to remain stable.

However, the speed at which information travels through the grid is complicated by the electric field. The electric field term in the density equations (equations (41a) - (41c)) is itself a function of density. This situation produces a feedback which acts to make the differencing scheme more sensitive to the time step than in the previous case (simple diffusion, no electric field). This feedback phemonena will be discussed in greater detail at a later time. However, it should be possible to put limits on the time step required. The speed of information in the grid should lie between the maximum velocity of the particles and the speed of light, c (the speed at which changes in the electric field occur). Therefore the upper limit on the time step (the largest possible time step) can be found by using the particle velocity in equation (36). The lower limit of the time step is calculated by substituting c into equation (36).

Development of Model Equations

We are now ready to begin the development of the equations which we will use to calculate the density profiles in a three component plasma. This discussion of the model equations development is divided into three areas: 1) boundary conditions; 2) momentum equations; 3) difference equations. For simplicity, we will develop the equations in a one dimensional (slab) geometry; however the development can be easily applied to other geometries. Therefore in our

development we will assume that the plasma is confined between to infinite parallel plates a distance 2L apart.

Boundary Conditions. As in the example above boundary conditions are applied to the particle fluxes. As before, we shall assume that the discharge is symmetric and therefore the flux of all three species is zero at the center. The flux condition on the wall for the electrons and negative ions is derived from basic transport theory (9:496). According to transport theory, the thermal flux on a completely absorbing boundary (which the wall is assumed to be) is given by $(1/4)n(L)\langle u\rangle$ (9:496). Where $\langle u\rangle$ is the average speed of the particle and n(L) is the density at the boundary.

In deriving the electron flux boundary condition, it is assumed the the average velocity of the electrons incident on the wall is given by their thermal velocity. Using the thermal velocity predicted by kinetic theory, $\langle u\rangle=(8k_BT_E/\pi m)^{1/2}$ (13:268), results in the following boundary condition on the electron flux:

$$\Gamma_E = n_E(L)(kT_E/2\pi)^{1/2} \qquad (42)$$

A phenomenon expression for the wall flux of the negative ions can be derived. Since the effect of the electric field, is to accelerate the negative ions toward the center of the discharge (where the field is weaker); the

characteristic velocity governing the negative ion flux at the wall, is the ions average thermal velocity. Therefore, we shall assume drift velocity of the negative ions is small compared to their thermal velocity. Therefore the wall flux for the negative ions is given by:

$$\Gamma_- = (n_- v_{Tb})/4 = n_-(L)(kT_-/2\pi)^{1/2} \quad (43)$$

In the case of the positive ions the Bohm criterion is applied. The Bohm criterion states that the ion velocity at the discharge boundary must be greater than or equal to the ion sound speed. The ion sound speed is given by (14:2487):

$$\langle u \rangle = [k(T_E + T_+)/m_+]^{1/2} \quad (44)$$

Because flux is equal to $n\langle u \rangle$, the following expression of the positive ion flux at the wall is obtained (note: we are not assuming a thermal flux and therefore, do not use $(n\langle u \rangle)/4$ as the wall flux expression):

$$\Gamma_+ = n_+(L)(k(T_E + T_+)/m_+)^{1/2} \quad (45)$$

Momentum Equations. With the derivation of the boundary conditions out of the way we can now begin to look at the development of the momentum equations. We will start with the general momentum equation (10):

$$mn\partial\langle\underline{v}\rangle/\partial t + mn(\langle\underline{v}\rangle\cdot\nabla)\langle\underline{v}\rangle + kT\nabla n - qEn = -mn\nu_{MT}\langle\underline{v}\rangle - m\langle\underline{v}\rangle S_{coll} \quad (10)$$

We will first consider the electron momentum equation. Like all the models reviewed, the inertial and collisional terms will be ignored. For a quasi-steady state the electron momentum equation yields:

$$\Gamma_E = D_E\partial n_E/\partial x - \mu_E E n_E \quad (46)$$

The positive ion momentum equation proved to be more complicated than the electron equation. The larger mass of the ion, coupled with a significant drift velocity (due to the electric field) makes it impossible to ignore the inertial and collisional terms. Because we expect the velocity of the positive ions to be mainly dependent on the electric field, the diffusive flux term ($kT\partial n/\partial x$) can be ignored. Ignoring the diffusive term and substituting $n_E z$ for S_{coll} reduces the steady state momentum equation for positive ions to:

$$\langle v_+\rangle\partial\langle v_+\rangle/\partial x = (eE/m_+) - \nu\langle v_+\rangle - (n_E z/n_+)\langle v_+\rangle \quad (47)$$

Equation (45) can be used to find an expression for calculating the positive ion velocity.

The mean free path for collisions between neutral gas atoms/molecules and positive ions is given by:

$$\lambda = 1/\langle N\sigma \rangle$$

where:

N is the neutral gas density

σ is the cross section for collisions.

Using the definition $\nu = N\sigma\langle v \rangle$ the expression for $\nu\langle v_+ \rangle$ can be rewritten in the following way:

$$\langle v_+ \rangle = N\sigma\langle v_+ \rangle^2 = \langle v_+ \rangle^2/\lambda \qquad (48)$$

Substituting equation (48) into equation (47) and rewriting $\langle v_+ \rangle \partial\langle v_+ \rangle/\partial x$ as $\partial(\langle v_+ \rangle^2/2)/\partial x$ yields:

$$\partial(\langle v_+ \rangle^2/2)/\partial x = eE/m_+ - \langle v_+ \rangle^2/\lambda - \langle v_+ \rangle z n_E/n_+ \qquad (49)$$

Finite differencing equation (49) gives:

$$(v_i^2 - v_{i-1}^2)/(2h) = eE_i/m_+ - v_i^2/\lambda - z v_i (n_E/n_+)$$

where $(n_E/n_+) = (n_{E,i+1} + n_{E,i})/(n_{+,i+1} + n_{+,i})$. This is the ratio of the electron to ion density (note the densities were averaged to approximate the density at the cell boundary were the flux and velocity are defined).

Collecting like terms and using the quadratic equation to

solve for v_i results in:

$$v_i^j = (-[\lambda' z(n_E^j/n_+^j)] + ([\lambda' z(n_E^j/n_+^j)]^2 + 4(\lambda'(eE^j/m + v_{i-1}^j/2h))^{1/2})/2 \quad (50)$$

where $\lambda' = 2h\lambda/(\lambda+2h)$. Using the boundary condition that $\langle v_{+,0}\rangle = 0$ (since $\Gamma = 0$ at $x=0$) the ion velocity at each cell boundary can be calculated by starting with $v_{+,1}$ and continuing to the wall. Using equation (50) for the ion velocity yields the following expression for the positive ion flux:

$$\Gamma_+ = (n_{+,i+1} + n_{+,i})v_i/2 \quad (51)$$

In deriving the negative ion momentum equation, it is assumed that the negative ion velocity will be dominated by its thermal velocity. Like Von Engel, therefore the inertial term $(\partial\langle v\rangle/\partial x)$ can be dropped. Then for a quasi-steady state, the negative ion momentum equation reduces to:

$$\nu_- \langle v_-\rangle = -eE/m_- - (kT_-/n_- m_-)\partial n_-/\partial x \quad (52)$$

Equation (52) can be rewritten as:

$$\Gamma_- = -D_-\partial n_-/\partial x - \mu_- E n_- \quad (53)$$

Difference Equations. With the flux expressions derived, it is now possible to look at the development of the difference equations which will be used to calculate the densities of the charged species. As in the development of equations (41a)-(41c), the first step is to finite difference the continuity equations and then substitute for the flux. The resulting expressions for the electron density are given by:

$$(n_{E,1}^{j+1} - n_{E1}^{j})/\tau = n_{E,1}^{j}(z-\alpha) + dn_{E,1}^{j} n_{-,1}^{j} - \{[-D_E/h](n_{E,2}^{j} - n_{E,1}^{j}) - (\mu_E/2)(n_{E,2}^{j} + n_{E,1}^{j})E_1^{j}\}/h \qquad i=1 \qquad (54a)$$

$$(n_{E,i}^{j+1} - n_{E,i}^{j})/\tau = n_{E,i}^{j}(z-\alpha) + dn_{E,i}^{j} n_{-,i}^{j} - \{[-D_E/h](n_{E,i-1}^{j} - 2n_{E,i}^{j} + n_{E,i+1}^{j}) - (\mu_E/2)([n_{E,i+1}^{j} + n_{E,i}^{j}]E_i^{j} - [n_{E,i} + n_{E,i-1}^{j}]E_{i-1}^{j})/h \qquad 2 \le i \le N-1 \qquad (54b)$$

$$(n_{E,N}^{j+1} - n_{E,N}^{j})/\tau = n_{E,N}^{j}(z-\alpha) + dn_{E,NN}^{j} n_{-,N}^{j} - \{(n_{E,NVTB}^{j}/4) + [D_E/h](n_{E,N}^{j} - n_{E,N-1}^{j}) + (\mu_E/2)(n_{E,N}^{j} + n_{E,N-1}^{j})E_{N-1}^{j}\}/h \qquad i=N \qquad (54c)$$

In their present form equations (54a)-(54c) can be solved for the electron densities in the next time step (j+1) (given the densities and electric field values from the j^{th} time step. However before doing this, it will be beneficial to examine the method employed by S. Rockwood in his solution of the Boltzmann transport equation for electron scattering (Reference 11).

Consider the form of equations (54a)-(54c) if the electric field and n_- were constants. If this were the case, equations (54a)-(54c) could be written in the form (11:2349):

$$n_i = \sum_{M=1}^{N} C_{i,M}\, n_M \tag{55}$$

where $C_{i,M}$ contains the coefficients on the right hand side of equations (54a)-(54c) (note that this includes the electric field and n_-; since, for the moment, we are assuming they are constants). If we now assume that the densities on the right side of equation (55) are in the (j+1) time step, it is possible to rewrite equation (55) in the form of a matrix equation (11:2349):

$$(\underline{I} - \tau\underline{C})n(t+\tau) = n(t) \tag{56}$$

where $\underline{I}$ is the identity matrix. One advantage of equation (56) is we can now solve for the densities implicitly. A second advantage is increased communication between cells is now possible, that is the cells are more effectively coupled together. These N coupled equations can now be solved by simple matrix methods.

In our case however, the electric field and n_- are not constants. The terms involving the electric field and n_- are non-linear terms (i.e., the consist of products of two

densities or the product of a density and a density dependent function). Because our only knowledge of the electric field and n_- is from the previous time step, the terms involving these values must remain in the j^{th} time step (and therefore on the right hand side of equation (56). The modified equation (56) is (11:2350):

$$(\underline{I} - \tau\underline{C}')\, n(t+\tau) = (\underline{I} + \tau\underline{T})\, n(t) \qquad (57)$$

where

$\underline{C}'$ is a constant matrix containing the coefficients of the linear terms of equations (54a)-(54c) and $\underline{T}$ is a tridiagonal matrix consisting of the non-linear terms. Since all of the values on the right hand side of equation (57) are known from the previous time step, the product of the right hand side of equation (57) is a vector (which we shall denote as $\underline{b}$). Letting $\underline{A} = (\underline{I} - \tau\underline{C}')$ the equation (57) can be rewritten as:

$$\underline{A}_E\, n(t+\tau) = \underline{b} \qquad (58)$$

Lets look now at equations (54a)-(55c) after employing Rockwood's solution method:

$$n_{E,1}^{j+1}(1-\tau(z-\alpha)+D_E\tau/h^2)-(D_E\tau/h^2)n_{E,2}^{j+1} = n_{E,1}^{j}(1+d\tau n_{-,1}^{j}) - (\tau\omega_E/2h)E_1^{j}(n_{E,1}^{j}+n_{E,2}^{j}) \qquad i=1 \qquad (59a)$$

$$n_{E,i}^{j+1}(1-\tau(z-\alpha)+2D_E\tau/h^2)-(D_E\tau/h^2)(n_{E,i+1}^{j+1}+n_{E,i-1}^{j+1})=$$
$$n_{E,i}^{j}(1+d\tau n_{-,i}^{j})-(\tau\nu_E/2h)\{E_i^j(n_{E,i+1}^{j}+n_{E,i}^{j})-$$
$$E_{i-1}^{j}(n_{E,i}^{j}+n_{E,i-1}^{j})\} \qquad 2 \le i \le N-1 \qquad (59b)$$

$$n_{E,N}^{j+1}(1-\tau(z-\alpha)+D_E\tau/h^2+\tau v_{TE}/h)-(D_E\tau/h^2)n_{E,N-1}^{j+1}= n_{E,N}^{j}(1+d\tau n_{-,N}^{j})$$
$$-(\nu_E\tau/2h)E_N^j(n_{E,N}^{j}+n_{E,N-1}^{j}) \qquad i=N \qquad (59c)$$

Similarly for the negative ions:

$$n_{-,1}^{j+1}(1-\tau\alpha)+D_-\tau/h^2)-(D_-\tau/h^2)n_{-,2}^{j+1}= n_{-,1}^{j}(1-d\tau n_{E,1}^{j})$$
$$-(\tau\nu_-/2h)E_1^j(n_{-,1}^{j}+n_{-,2}^{j}) \qquad i=1 \qquad (60a)$$

$$n_{-,i}^{j+1}(1-\tau\alpha)+2D_-\tau/h^2)-D_-\tau/h^2(n_{-,i+1}^{j+1}+n_{-,i-1}^{j+1})= n_{-,i}^{j}(1-d\tau n_{E,i}^{j})$$
$$-(\tau\nu_-/2h)[E_i^j(n_{-,i+1}^{j}+n_{-,i}^{j})- E_{i-1}^{j}(n_{-,i}^{j}+n_{-,i-1}^{j})]$$
$$2 \le i \le N-1 \qquad (60b)$$

$$n_{-,N}^{j+1}(1-\tau\alpha)+D_-\tau/h^2+(\tau v_{TE}/4h))-(D_-\tau/h^2)n_{-,N-1}^{j+1}= n_{-,N}^{j}(1-d\tau n_{E,N}^{j})$$
$$-(\nu_-\tau/2h)E_N^j(n_{-,N}^{j}+n_{-,N-1}^{j}) \qquad i=N \qquad (60c)$$

Substitution of the positive ion flux expression (equation (51)) into the positive ion continuity equation (equation (8)) yields:

$$n_{+,i}^{j+1}=n_{+,i}^{j}+z\tau n_{E,i}^{j}-(\tau/h)(n_{+,i}^{j}v_i^j-n_{+,i-1}^{j}) \quad 2 \le i \le N-1 \qquad (61a)$$

Where v_i^j is the positive ion drift velocity given by equation (50). Applying the boundary conditions to obtain

$n_{*,1}$ and $n_{*,N}$ we get:

$$n_{*,1}^{j+1}=n_{*,1}^{j}+z\tau n_{E,1}^{j}-(\tau/h)n_{*,1}^{j}v_1^{j} \qquad i=1 \tag{61b}$$

$$n_{*,N}^{j+1}= n_{*,N}^{j}+z\tau n_{E,N}^{j}-(\tau/h)(n_{*,N}^{j}v_{ss} - n_{*,N-1}^{j}v_{N-1}^{j}) \tag{61c}$$

where v_{ss} is the ion sound speed (equation (44)). With the exception of the $z\tau n_E$ term, equations (61a)-(61c) are made up of only non-linear terms (because v_i^j is a function of density). Therefore we can not apply Rockwood's method for calculating the the positive ion densities. All of the values on the right hand side of equations (61a)-(61c) are known from the previous time step. Therefore it is possible to calculate the positive ion density by direct substitution.

Code Operation

Let's look now at how the equations developed above are used in a computer code to calculate the charged particle distributions and their associated electric field. Looking at the basic algorithm will make it easier to understand the operation of the code. The basic steps of the algorithm are:

1) Input the initial densities and electric field (usually based on Schottky theory).

2) Perform a LU decomposition on the "A" matrix of both species (i.e. break the A matrix into Upper and Lower Diagonal matrices) .

3) Calculate the "b" vector of the electrons and negative ions and solve for their densities by using back substitution.

4) Calculate the positive ion velocity for each cell boundary.

5) Using the velocities, find the positive ion density for each cell.

6) Using the charged particle densities, calculate the electric field.

7) Return to step 3. Repeat this process until the solution converges to steady state.

Let's now look at each of these steps in more detail. As we see, the first step is to input the initial densities and electric field. These are the values the code will use as the old values (i.e. zeroth time step) in the first time step. For our runs in the two component case the ambipolar profiles were used as the initial parameters.

To solve the matrix equations a LU decomposition is performed on the A matrices of both species. Since these matrices are constants, the LU decompositions must be performed only once by the code. The LU decomposition is performed by a subroutine called LUDECOMP taken from Reference 10. With these decompositions completed the code begins the first time step.

Using the densities and electric fields from the previous time step (the initial values for the first time step), the b vectors are calculated. The densities are then solved for using back substitution. This function is performed by a subroutine called LUBKSB, also taken from Reference 10. (This is actually a two step method in that the operation is performed first on the electrons and then on the negative ions).

As mentioned in the development section, the positive ion equation is composed only of non-linear terms so it is impossible to apply the matrix method to solve for its densities. To calculate the positive ion densities, the code must first calculate the ion velocity for each cell boundary. To do this, the code uses a DO loop and equation (50). Because the velocity at the center (v_0) is zero, equation (50) can be used as a recursion relation for the positive ion velocity. The velocities for all cell boundaries up to v_{N-1} (the left boundary of the last cell) are calculated in this way. The wall velocity v_N is taken care of by the wall flux boundary condition. With these velocities calculated the code then uses equations (61a)-(61c) to calculate the cell densities. Like the velocity calculations this is done on a cell-by-cell basis using a DO loop.

Now that the code has calculated all of the new charged particle densities, the updated electric field can be calculated. As in the illustrative example in the beginning

of this section, the electric field is calculated using a expression derived from Poisson's equation. In this case, the electric field expression is:

$$E_i^j = (e/\varepsilon_0) \sum_{M=1}^{i} (n_{+,M}^j - n_{E,M}^j - n_{-,M}^j)h$$

The calculation of the electric field marks the end of the time step. At this point the code increments the time and returns to the third step (calculation of the b vectors). This procedure is repeated until the density profiles reach steady state. The following criteria will be used to determine when the profiles have reached the steady state. We shall assume that a steady state exists when the positive ion density changes less than 1% over a time span equal to ten characteristic diffusion times. For our preliminary runs, we will limit the time iterations by establishing a time loop counter. When the loop counter reaches a set value the program will terminate. The purpose for doing this it to allow us to monitor the code operation in the early "checkout phase" of the code. At run termination the code writes the charged particle densities and electric field to an output file called "fdif.res". A complete listing of the code is included in Appendix C. An outline of the input data is also covered in Appendix C.

V. Results and Discussion

Up to this point we have only been concerned with the development of the model. We want to now turn our attention to whether or not this model correctly predicts the behavior of a real plasma. Our initial plans called for testing the code in phases: 1) one component diffusion; 2) two component plasma; 3) three component (one dimensional slab); 4) three component (cylindrical). The purpose for dividing the code testing into four phases is to allow the code behavior to be monitored and refined in problems of increasing complexity. Unfortunately, computational difficulties arose while testing the code in the two component phase; therefore, the discussion in this chapter will be limited to the first two phases. The third and fourth phases will be discussed in the final chapter of this paper.

Phase One

Phase one is the testing of the code in a one dimensional diffusion problem. Our system in this problem consists of of one species of neutral particles. This simple case will allow us to see if the code is capable of modeling a diffusion problem in which only density driven diffusion exists (ie. no electric field). It will be assumed that the particles obey the continuity equation (37) and flux equation equation (38) (minus the electric field

terms); therefore, the code will be calculating solutions of the equation:

$$\partial n/\partial t = D_E(\partial^2 n/\partial t^2) + zn \qquad (62)$$

To determine the behavior of the model, this one component system will be tested for three different cases. These case are: 1) no production and leakage; 2) non-zero leakage and no production; 3) non-zero leakage and production. For each of these cases, we shall assume that the initial density profile is a cosine function with a maximum at the center (x=0) and a minimum at the wall. To determine if the code is properly modeling the problem, the code's results will be compared to analytic solutions.

Lets look briefly at the expected results of the three cases. For case one (no production or leakage), the steady state density profile is apparent. Because no production or losses occur in this case, the density profile will become uniform in time (i.e., the density in each cell will be the same).

For case two (losses with no production), lets look at the solution to equation (62) derived in Appendix B.

$$n(x,t) = n_0 \exp[(z - D\cdot^2)t]\cos(\cdot x) \qquad (B\text{-}10)$$

where $\cdot$ is the root of equation (B-7) (i.e., an eigenvalue). The loss in this case is due to removal of particles at the

boundary wall. This loss is given by: $(n(L)v/4)$, where v is the velocity of the particles at the wall. In this case the production term (z) is zero; therefore equation (B-10) predicts that the density profile will be a cosine function decaying in time.

We again turn to equation (B-10) in evaluating the third case. In this case we will choose a z that makes the exponent in equation (B-10) zero, i.e., the steady state solution. From this case we will be able to determine if the code is capable of reaching a steady state solution in a problem in which particles are being both lost and created.

The code produced the expected results for each of the three cases. Since the profiles of cases one and two are uninteresting (i.e., flat and zero, respectively), we will only discuss the case three results in detail. A comparison of the code predicted profile and the analytic solution is shown in Figure 7. Plotted is the normalized density versus the cell number for a steady state solution (with $D_E = 5.17 \times 10^5$ cm^2/sec; $z = 1.195 \times 10^6$ sec^{-1}; [eq. (B-7), L=1] $= 1.517$). The analytic solution densities were calculated at the right hand side of the cells (i.e., at $x = .1, .2, .3, \ldots, 1$). As can be seen from Figure 7, the code and solution results are in close agreement. The largest difference occurs in cell 7, with a percent difference of 4.3% .

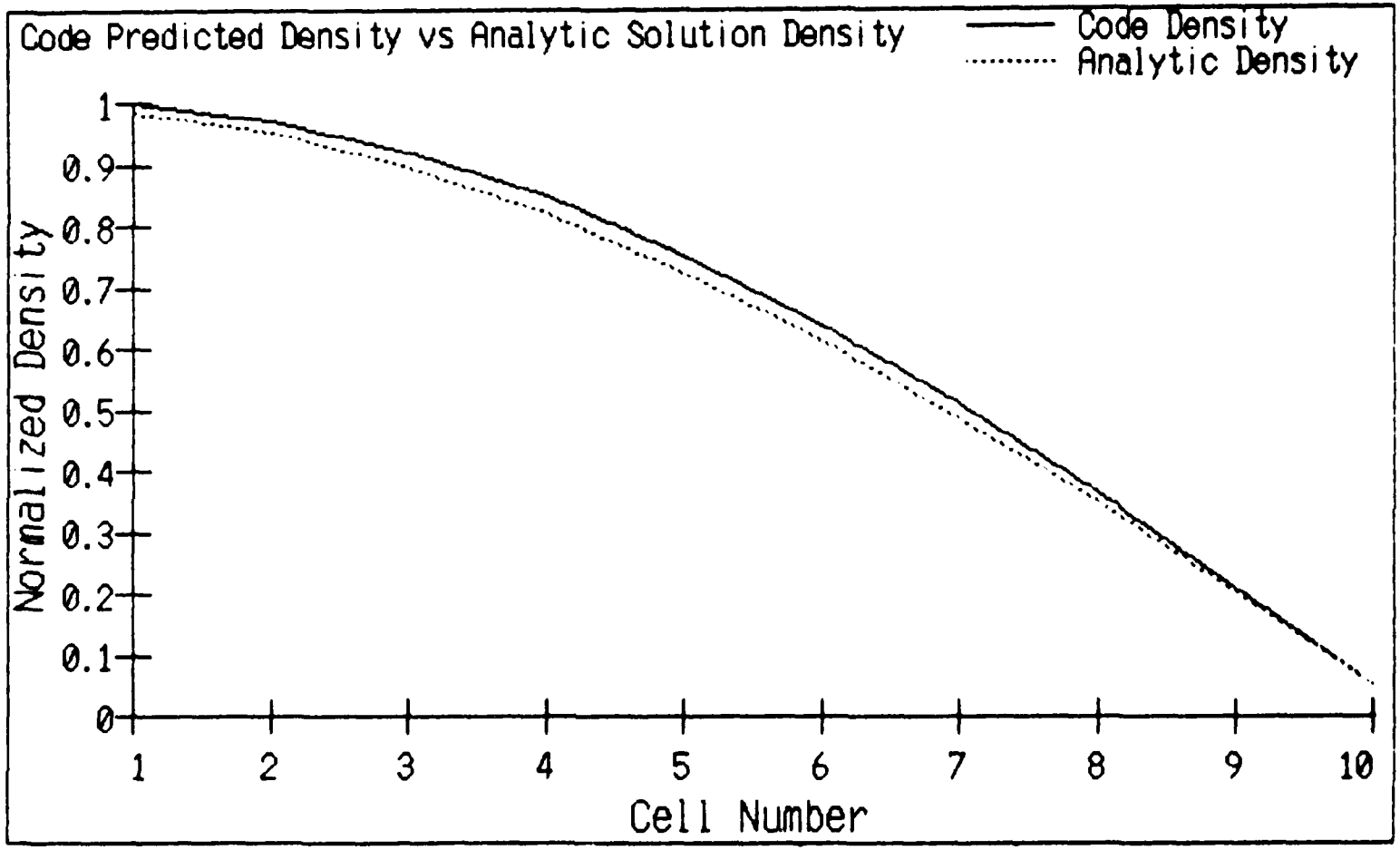

Figure 7. Comparison of Model Code and Analytic Solution for One Component Diffusion Problem

An unexpected result of this phase was that of code sensitivity to round-off error. Attempts to run the model with single precision variables resulted in crashes of the computer code. This problem was corrected by performing the calculations with double precision variables.

Phase Two

Having successfully completed the first phase, testing of the code for the two component plasma began. The purpose of this step is to increase the complexity of the problem and test the behavior of the code. As phase one, we have only one loss and source process; however, we now have the additional features of an electric field-driven flux and coupling of two oppositely charged species by the electric field.

One item of particular interest in this phase will be the effect of the electric field on numerical instability. The addition of the electric field will make the plasma equations (finite differenced continuity and momentum equations) sensitive to the choice of time step. By looking at the time scales of the electrons and ions (or more appropriately the difference between the time scales) it is possible to understand how the electric field sensitizes the plasma equations. The particle's time scale is the characteristic time in which the species reacts to changes in the electric field and density gradients. The electron time scale is short compared to that of the ions. Therefore

during a large time step, the electron density can change greatly over that of the ions. This, in turn, can cause large changes in the electric field. These field changes are then fed back into the density calculations of the next time step. The overall results of a large time step can be erratic density and electric field profiles.

As in the first phase the code results will be compared with another solution to determine if the model/code is correctly modeling the plasma. We will use Self and Ewald's model as the comparison solution in this phase. Self and Ewald's model is ideal for this comparison for three reasons. The first reason is that Self and Ewald's solution, like our model, is in slab geometry. Therefore a more direct comparison can be made using this model. The second reason is that the boundary conditions applied by Self and Ewald are similar to ours, i.e., the Bohm criterion is applied for the ions at the wall. The third reason is that the results of Self and Ewald's model can be easily compared for different ionization rates. This makes it possible to test our model in different cases, as was done in the first phase.

In phase one we simply varied the source rate to develop the different cases in which the code was tested. In this phase we will indirectly vary the source rate (ionization) by testing the code in different background gas pressures (the ionization rate is proportional to the neutral density which is dependent on the gas pressure).

This can best be understood by a quick review of Self and Ewald's solution. The density profile predicted by Self and Ewald's model is strongly dependent on the pressure of the background gas. This can be easily seen in Figure 2, where the density profiles for several different pressures are plotted. In this plot the pressure dependence is represented by the pressure parameter (A) (14:2487). A is the ratio of the ionization rate to the sum of the ioniztion rate (z) and ion-neutral collision frequency (ν). For low pressure gases the ion-neutral collision frequency is small so the pressure parameter is approximately unity. Therefore a low pressure gas is a gas in which the mean free path for collisions between ions and neutrals is large compared to the discharge tube radius (14:2487). Just the opposite is true in a high pressure gas. In a high pressure gas A approaches zero and the mean free path of ion-neutral collisions is much greater than the tube radius.

The three particular cases we will look at are $A \approx 1$ ($\nu \ll z$), $A = .5$ ($\nu = z$), $A \approx 0$ ($\nu \gg z$). In the low pressure case the density profile should be approximately that of the profile predicted by the free fall theory (14:2486), see Figure 2. The second case is an intermediate pressure and the expected profile lies between that of the free fall and ambipolar profiles. The last case, $A \approx 0$, is a high pressure case. The expected profile is like that of the ambipolar case (14:2486).

As was expected, the code was sensitive to the magnitude of the time step interval. It was found that when using ten cells to model the plasma, the time step had to less than or equal to 10^{-8} seconds for the code to remain numerically stable. When using 100 cells the time interval was restricted to less than 10^{-10}. These restraints forced long computational times (e.g., to bring the real time calculation of the ten cell model to one millisecond required 100,000 time steps).

In all attempts to calculate the densities of the two component plasma, the positive ion density became ionization as the integration in time progressed. This is best demonstrated by the positive ion profile evolution depicted in Figure 8. The resulting electric field profile is shown in Figure 9.

From Figure 8 we see that the ion density becomes increasingly erratic as the integration in time progresses. We note that an oscillation first becomes apparent at 50 sec. This oscillation then spreads inward toward the axis. Allowing the calculations to progress further in time resulted in negative densities being predicted; therefore, we are assured that this behavior is code generated and not real.

The cause of the numerical instability (oscillations) was not discovered during the course of the research. During the writing of this report, code errors were discovered in the ion velocity calculations. These errors

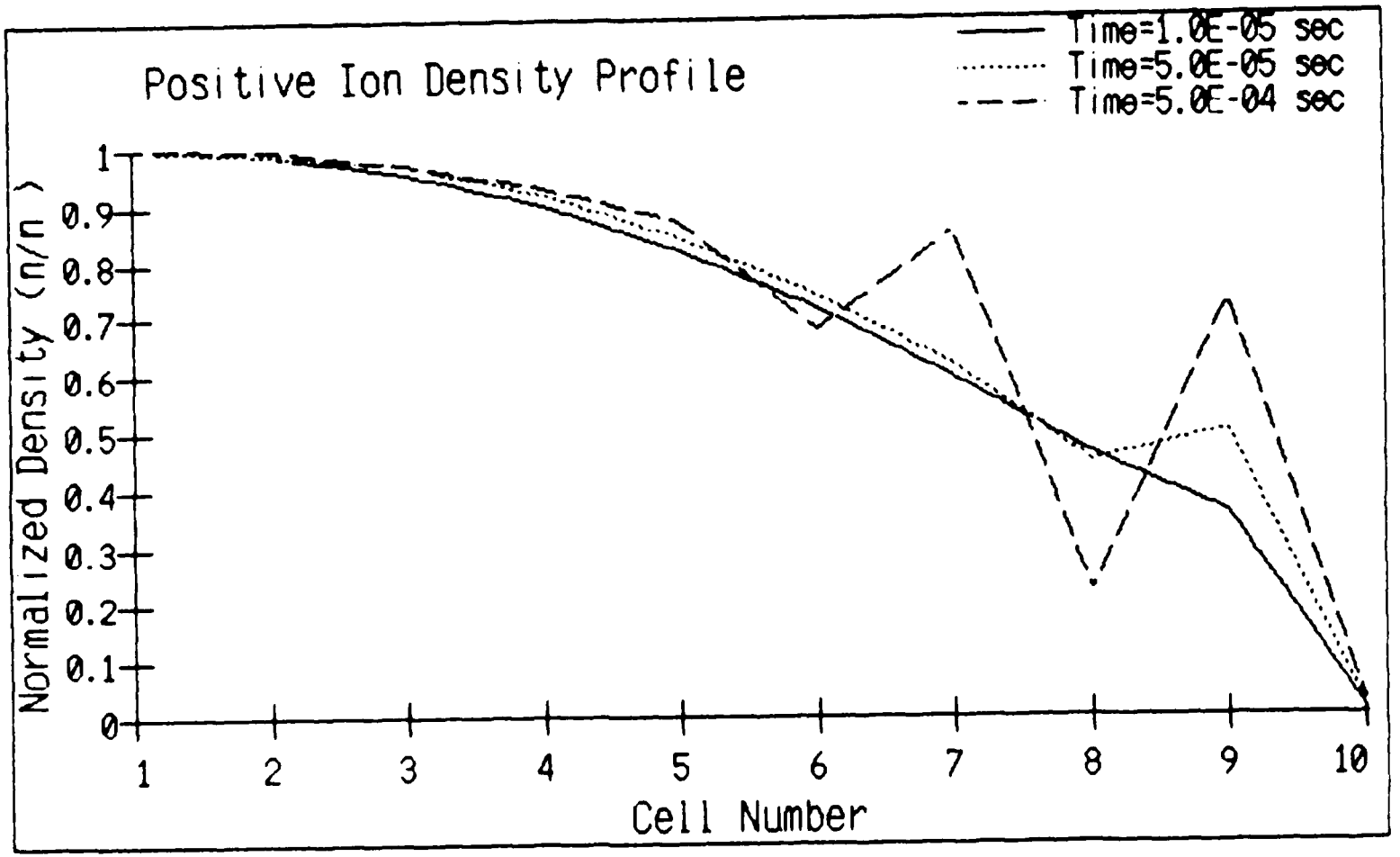

Figure 8. Time Evolution of Positive Ion Profile

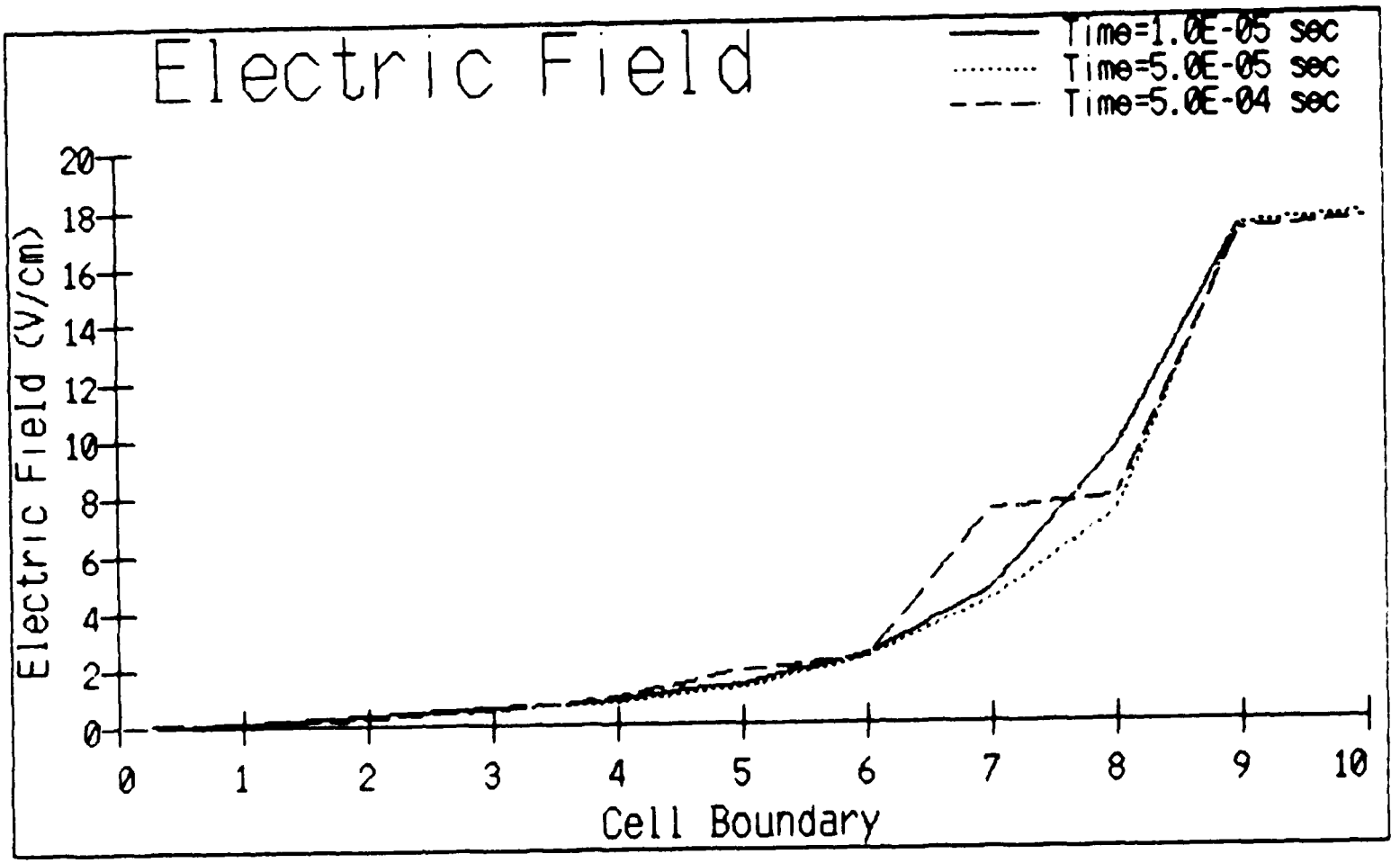

Figure 9. Time Evolution of Electric Field

were at least in part the cause for the oscillations seen in the code results. A detailed analysis of the results of the corrected code was not possible due to time limitations. A quick examination of the ion velocities revealed that a inconsistency existed at the discharge wall. The velocity on the left edge of the last cell (cell boundary before wall) was greater than the ion sound speed (by a factor of four in one case). This inconsistency led to a "pile-up" in the last cell of the grid, which in turn led to oscillations in the ion densities. This behavior implies that our boundary condition for the positive ions (i.e., the ion velocity at the wall is exactly equal to the ion sound speed) is invalid.

VI. Conclusions and Recommendations

In this chapter we shall discuss some of the areas which should be explored in an attempt to correct the current problems experienced in the model and code. We will also discuss the final two phases of the code testing, which could be undertaken once the current problems are corrected and phase two testing completed.

Model/Code Corrections

The first area which must be researched, before code testing can continue, is the boundary condition on the positive flux at the discharge wall. In particular, the effect of allowing the ion's wall velocity to exceed the ion sound speed should be examined. As an alternative to fixing the positive ion velocity at the wall, to the ion sound speed, is to use equation (50) to calculate the ion speed at the wall.

The second area which should be examined is that of the sensitivity of the code to the time step. Because the electric field coupling is the primary cause of this sensitivity, it may be possible to reduce this sensitivity by by introducing a perturbation term to the electric field. The new form of the electric field would be:

$$E(x,t) = E_0(x) + E_1(x,t)$$

where E_0 is a time constant field term, based on the expected electric field profile. For example in the case of the two component plasma, E_0 would be a Tangent function, as predicted by the ambipolar theory. The perturbation E_1 would be the difference between the field calculated using Poisson's Equation and E_0. Therefore all changes in the electric field from one time step to the other would be contained in the perturbation term. We would expect this perturbation term to be small; therefore, a larger time step should be possible.

This change will also better couple the electric field into the density calculations. This coupling can be seen by substituting this new electric field expression in the electron and negative ion density equations (equations ((59a)-(59c) and (60a)-(60c)). Currently the electric field terms are retained on the right hand side of these equations (because the are non-linear terms). By writing the electric field with a constant and a perturbation it will be possible to bring the E_0 terms to the left hand side of the equations. Substituting for the electric field yields the following for the electrons:

$$n_{E,1}^{j+1}(1-\tau(z-\sigma)+(D_E\tau/h^2)+(\mu_E\tau/2h)E_{0,1})-((D_E\tau/h^2)+(\mu_E\tau/2h)E_{0,1})n_{E,2}^{j+1}= n_{E,1}^{j}(1+d\tau n_{-,1}^{j})-(\mu_E\tau/2h)\{E_{1,1}^{j}(n_{E,1}^{j}+n_{E,2}^{j})\} \qquad i=1 \qquad (63a)$$

$$n_{E,1}^{j+1}\{1-\tau(z-\alpha)+(2D_E\tau/h^2)+(\mu_E\tau/2h)(E_{o,1}-E_{o,1-1})\}-$$
$$n_{E,1-1}^{j+1}([\mu_E\tau/2h]E_{o,1-1}+[D_E\tau/h^2])+n_{E,1+1}^{j+1}([\mu_E\tau/2h]E_{o,1+1}-$$
$$[D_E\tau/h^2])=n_{E,1}^{j}(1+d\tau n_{-,1}^{j})-(\mu_E\tau/2h)\{E_{1,1}^{j}n_{E,1}^{j}-E_{1-1}^{j}n_{E,1-1}^{j}\}$$
$$i\le i \le N-1 \qquad (63b)$$

$$n_{E,N}^{j+1}\{1-\tau(z-\alpha)+(D_E\tau/h^2)+(\mu_E\tau/2h)E_{o,N}+\tau v_{TE,E}/h\}+n_{E,N-1}^{j+1}([\mu_E\tau/2h]$$
$$-[D_E\tau/h^2])=n_{E,N}^{j}(1+d\tau n_{-,N}^{j})-(\mu_E\tau/2h)E_{1,N}^{j}(n_{E,N}^{j}+n_{E,N-1}^{j})$$
$$i=N \qquad (63c)$$

Similarly for the negative ions:

$$n_{-,1}^{j+1}[1-\tau\alpha+(D_E\tau/h^2)+(\mu_-\tau/2h)E_{o,1}]-\{(D_-\tau/h^2)+$$
$$(\mu_-\tau/2h)E_{o,1}\}n_{-,2}^{j+1}=n_{-,1}^{j}(1-d\tau n_{E,1}^{j})-(\mu_-\tau/2h)\{E_{1,1}^{j}$$
$$(n_{-,1}^{j}+n_{-,2}^{j})\} \qquad i=1 \qquad (64a)$$

$$n_{-,1}^{j+1}\{1-\tau\alpha+(2D_-\tau/h^2)+(\mu_-\tau/2h)(E_{o,1}-E_{o,1-1})\}-$$
$$n_{-,1-1}^{j+1}([\mu_-\tau/2h]E_{o,1-1}+[D_-\tau/h^2])+n_{-,1+1}^{j+1}([\mu_-\tau/2h]E_{o,1+1}-$$
$$[D_-\tau/h^2])=n_{-,1}^{j}(1-d\tau n_{E,1}^{j})-(\mu_-\tau/2h)\{E_{1,1}^{j}n_{-,1+}^{j}-E_{1-1}^{j}n_{-,1-}^{j}\}$$
$$i\le i \le N-1 \qquad (64b)$$

$$n_{-,N}^{j+1}\{1-\tau\alpha+(D_-\tau/h^2)+(\mu_-\tau/2h)E_{o,N}+\tau v_{TE,-}/h\}+n_{-,N-1}^{j+1}([\mu_-\tau/2h]-$$
$$[D_-\tau/h^2])=n_{-,N}^{j}(1-d\tau n_{E,N}^{j})-(\mu_-\tau/2h)E_{1,N}^{j}(n_{-,N}^{j}+n_{-,N-1}^{j})$$
$$i=N \qquad (64c)$$

where $n_{s,1+}^{j}=(n_{s,1}^{j}+n_{s,1+1}^{j})$; $n_{s,1-}^{j}=(n_{s,1}^{j}+n_{s,1-1}^{j})$.

Future Testing

Once the two areas discussed above have been addressed, it will possible to continue the testing of the code, as outlined in phase two. In this section we will discuss the code testing which should occur after the phase two testing is complete.

Having successfully completed phase two, we will have proved the finite differencing method's ability to model a simple plasma. Therefore our primary goal in the third phase is to establish the general density profiles of the three component plasma for different sets of parameters (i.e., different ionization, attachment, and detachment rates). A secondary goal will be to compare the code's results with Lee's and Von Engel's solutions to verify the relationships among the particle densities (i.e., greater positive ion densities than electron densities throughout the volume, negative ions confined to the axis region, etc.) reported in their papers.

Though we cannot expect profiles identical to Von Engel's or Lee's since their results are in cylindrical geometry, a comparision of our model's results with their results should be possible. The basic relationships between the profiles of the different species should be comparison in both geometries. From this comparison it may be possible to draw conclusions on the accuracy or inaccuracy of their models.

The last phase of the testing will be to cast the model into cylindrical geometry. The purpose of this phase is to make the model more realistic by making it "two dimensional". A second advantage of this phase is that now a direct comparison of the solutions of Lee and Von Engel can be made.

Conclusions

Despite the problems encountered in the research the finite differencing method still appears to be a viable method for modeling a plasma. Research should continue to discover the problems in the existing model, with special attention given to the ion velocity calculations and boundary conditions. Once the instability (oscillation) problem is overcome, I believe significant results can be achieved with this approach.

APPENDIX A

Development of Self and Ewald's Plasma Model

The authors start with the following steady state continuity and momentum equations:

$$\nabla\cdot(n\mathbf{v})=G \tag{A-1}$$

$$n(\mathbf{v}\cdot\nabla)\mathbf{v}+G\mathbf{v}=(nq/m)\mathbf{E}-(\nabla\cdot\Phi/m)-n\nu\mathbf{v} \tag{A-2}$$

where:

ν is the collision frequency for momentum transfer;

G is the volumetric production rate;

Φ is the pressure tensor.

Making the following substitutions:

$$\nabla\cdot\Phi=kT\nabla n \tag{A-3}$$

$$G=\nu_I n_\varepsilon \tag{A-4}$$

Where ν_I is the ionization frequency. Equation (A-1) can be rewritten by substituting (A-4) into (A-1):

$$\mathbf{v}(\nabla\cdot n)+n(\nabla\cdot\mathbf{v})=\nu_I n$$

$$\mathbf{v}(\nabla\cdot n)(1/n)+\nabla\cdot\mathbf{v}=\nu_I$$

$$\mathbf{v}\cdot\nabla[\mathrm{Ln}(n)]+(\nabla\cdot\mathbf{v})=\nu_I \tag{A-5}$$

Substituting (A-3) in (A-2) yields:

$$n(\mathbf{v}\cdot\nabla)\mathbf{v}+n\nu\mathbf{v}=nq(\mathbf{E}/m)-(kT/m)\nabla n-n\nu\mathbf{v}$$

dividing by n and letting $\nu' = \nu_I + \nu$ gives

$$(v\ \nabla)v = q(E/m) - (kT/m)\nabla[Ln(n)] - \nu' v \qquad (A\text{-}6)$$

In one dimensional slab geometry (discharge between to infinite parallel plates, equation (A-5) reduces to:

$$dv/dr + v\ d[Ln(n)]/dr = \nu_I \qquad (A\text{-}7)$$

where r is the spatial variable. Substituting $E = -\nabla\phi$ for the electric field and -e for q in equation (A-6) yields the momentum transfer equation for the electrons:

$$v\ dv/dr = (e/m_E)d\phi/dr - (kT_E/m_E)\ d[Ln(n)]/dr - \nu_E' v \qquad (A\text{-}8)$$

similarly for the ions

$$v\ dv/dr = -(e/m_+)d\phi/dr - (kT_+/m_+)\ d[Ln(n)]/dr - \nu_+' v \qquad (A\text{-}9)$$

Note that the author assume quasi-neutrality and therefore make no distinction in the density variable (i.e., $n=n_E=n_+$).

Equations (A-7)- (A-9) are normalized using the following factors.

$$\tau = e\phi/kT_E \ ;\ u = (m_+/kT_E)^{1/2}\ v \ ;\ s = (m_+/kT_E)^{1/2}\ \nu_+'\ r \ ;$$
$$R' = (m_+/m_E)(\nu_+'/\nu_E') \ ;\ A = \nu_I/\nu_+' \ ;\ \tau = T_+/T_E \qquad (A\text{-}10)$$

Using the chain rule yields an expression for d /dr

$$d/dr = (m_e/kT_E)^{1/2} \nu_+ d/ds \qquad (A-11)$$

Direct substitution of (A-11) and (A-10) in equation (A-7) yields the normalized continuity equation:

$$d(u)/ds + u\, d[Ln(n)]/ds = A \qquad (A-12)$$

Before normalizing the electron momentum transfer equations the authors assume that the electron inertial term can be ignored due to the small mass of the electron (14:2487). Now performing the normalization gives:

$$u = R'(d\Gamma/ds) - \tau\, d[Ln(n)]/ds \qquad (A-13)$$

Normalization of the ion equations yields:

$$u + u(du/ds) = -d\Gamma/ds - \tau\, d[Ln(n)]/ds \qquad (A-14)$$

The authors' next step is to make u the independent variable in equations (A-12)-(A-14). The chain rule is used to obtain an expression for d/ds. This expression is substituted into equations (A-12)-(A-14) yielding:

$$1 + u\, d[Ln(n)]/ds = A\, ds/du \qquad (A-15)$$

$$u\, ds/du = R'(d\Gamma/du - d[Ln(n)]/du) \qquad (A-16)$$

$$u(1 + ds/su) = -d\bar{\tau}/du - \tau\, d[Ln(n)]/du \qquad (A\text{-}17)$$

Equations (A-15)- (A-17) are now solved to find ds/su, s, $Ln(n/n_0)$, and $\bar{\tau}$ (n_0 is the density at x=0). Solving (A-16) for $d\bar{\tau}/ds$ we find:

$$d\bar{\tau}/ds = (u/R')ds/du + d[Ln(n)]/du \qquad (A\text{-}18)$$

Substituting (A-18) for $d\bar{\tau}/ds$ in (A-17) yields:

$$d[Ln(n)]/du = (A/u)ds/du \qquad (A\text{-}19)$$

(A-19) can now be used in (A-15) to solve for ds/du .

$$ds/du = [(1+\tau)-u^2]/[A(1+\tau)+(1+1/R')u^2] \qquad (A\text{-}20)$$

(A-20) is integrated to find s.

$$s=[(1+\tau)^{1/2}(1+1/R'+A)]/[A^{1/2}(1+1/R')^{3/2}]\mathrm{Tan}^{-1}(Wu)-u/(1+1/R') \qquad (A\text{-}21)$$

where $W=[(1+1/R')/(A(1+\tau))^{1/2}]$.

Integration of (A-19) (note: n(0)=0) yields

$$Ln(n/n_0)=-[1+1/R'+A]/[2(1+1/R')]Ln(Y) \qquad (A\text{-}22)$$

where $Y=[(1+1/R')u^2+A(1+\tau)]/[A(1+\tau)]$. (A-18) is integrated to yield an expression for the normalized potential .

$$\eta = -[(1-\tau/R')(1+1/R'+A)]/[2(1+1/R')^2]\mathrm{Ln}(Y)-u^2/[2(1+R')] \qquad (A-23)$$

APPENDIX B

Development of the Solution for One Component Diffusion

This appendix outlines the development of the solution for one species diffusion in one dimension. The system consists of two infinite parallel plates separated a distance 2L . It is assumed that the particles conservation is governed by the following continuity equation:

$$\partial n/\partial t = -(\nabla \cdot \Gamma) + zn \qquad (B\text{-}1)$$

where z is the particle production rate. It is further assumed that the particle flux can be expressed by Fick's Law:

$$\Gamma = -D\nabla n \qquad (B\text{-}2)$$

where D is a constant diffusion coefficient.

As a boundary condition, it is assumed that the flux at the wall (i.e., the particle loss) is given by:

$$\Gamma(L) = (n(L)v)/4$$

where v is the average velocity of the particles.

Casting equations (B-1) and (B-2) in cartesian coordinates and substituting (B-2) into (B-1) yields:

$$\partial n/\partial t = D\partial^2 n/\partial x^2 + zn \qquad \text{(B-3)}$$

Applying the method of separation of variables we assume that $n(x,t)=X(x)T(t)$. Substituting for n in equation (B-3) gives the following expression:

$$X(x)\partial T(t)/\partial t = DT(t)\partial^2 X(x)/\partial x^2 + X(x)T(t)z$$

or

$$(1/D)[T'(t)/T(t)] - (z/D) = X''(x)/X(x)$$

The only way for this equality to be true is for both sides of the equation to be equal to a constant (ν). Therefore we get to separate equations.

$$X''(x)/X(x) = \nu \qquad \text{(B-4)}$$

$$(1/D)\{[T'(t)/T(t)] - z\} = \nu \qquad \text{(B-5)}$$

Expanding (B-4) we get the following:

$$X''(x) = \nu X(x)$$

Before we can solve this differential equation we must establish the boundary conditions for the separated equations. The first boundary condition comes from the boundary condition of the flux at x=0, i.e., $\Gamma(0,t)=0$. If the flux at x=0 is zero then $-DT(t)X'(x)=0$. Since this must hold true for all times $X'(0)=0$. Similarly the boundary condition on the flux at x=R yields that $X'(R)=-(v/4D)X(R)$.

Now we can begin to solve the differential equations above. The first step is to determine if the constant λ is negative, positive, or zero. Assuming first that λ is positive and that $\lambda=\alpha^2$. Using this in the differential equation we find that the solution is:

$$X(x)= A_1\exp(-\alpha x) + A_2\exp(\alpha x)$$

Taking the derivative of this solution gives

$$X'(x) = -A_1\alpha\exp(-\alpha x) + A_2\alpha\exp(\alpha x)$$

From the boundary condition at x=0 we find that $A_1=A_2$. Substituting for A_2 and applying the boundary condition at x=L yields:

$$A_1\alpha[\exp(-\alpha L) - \exp(\alpha L)]= -(v/4D)A_1[\exp(-\alpha L) + \exp(\alpha L)]$$

Therefore, $\alpha=-(v/4D)(1/\tanh(\alpha R))$; however, there are no roots to this equation. Therefore, $\lambda>0$ is not a possible solution.

A second possible solution is that $\lambda=0$. Applying this we get:

$$X(x)= A_1x + A_2$$

and

$$X'(x) = A_1$$

Applying the boundary condition at the x=0 tell us A_1 must be zero. If $A_1 = 0$ then the boundary condition at the wall can not be met.

The only choice left is that λ is negative. Assuming $\lambda=-\lambda$ we get:

$$X(x)= A_1\cos(\sqrt{\lambda}x) + A_2\sin(\sqrt{\lambda}x) \qquad \text{(B-6)}$$

and

$$X'(x)= -A_1\sqrt{\lambda}\sin(\sqrt{\lambda}x) + A_2\sqrt{\lambda}\cos(\sqrt{\lambda}x)$$

Because $X'(0)=0$, A_2 must be zero. Using this and applying the wall boundary condition yields:

$$-A_1\sqrt{\lambda}\sin(\sqrt{\lambda}L) = -(\nu/4D)A_1\cos(\sqrt{\lambda}L)$$

Therefore λ is given by $\lambda=(\nu/4D)\cot(\sqrt{\lambda}R)$. This relation has possible roots and thus is our solution.

$$X(x)= A_1\cos(\sqrt{\lambda}x) \quad \text{where } \lambda=(\nu/4D)\cot(\sqrt{\lambda}R) \qquad \text{(B-7)}$$

Turning our attention to the the time dependent equation we find:

$$T'(t) - (z-D\lambda^2)T(t) = 0$$

The solution to this equation is

$$T(t) = \exp([z-D\lambda^2]t) \qquad (B-8)$$

Since $n(x,t)=X(x)T(t)$ we get for our finial solution

$$n(x,t)= A_1\{\exp([z-D\lambda^2]t)\cos(\lambda x)\} \qquad (B-9)$$

Defining the density at $t=0$ and $x=0$ as n_o we can evaluate A_1, i.e., $n(0,0)=n_o$, so

$$n(x,t)=n_o\{\exp([z-D\lambda^2]t)\cos(\lambda x)\} \qquad (B-10)$$

where λ is the roots of $\lambda=(v/4D)\cot(\lambda L)$. It should be noted that this solution also can be used as a solution to the ambipolar model if we substitute D_A for D.

APPENDIX C

Finite Difference Model Code

This appendix is a listing of the latest computer code used in the research. The program requires input from a data file called fdif.dat. The data in fdif.dat is as follows:

ts - # of time steps to perform

c - # of cells in grid

D_e- Electron Diffusion Coef.

μ - Electron Mobility

T_e,T_+- The electron and ion temperatures in Kelvin

σ - The ion-neutral collision cross section

z - Ionization rate

m_+- Ion mass

s - k/h ratio of time step interval to cell width

α - Attachment rate

d - Detachment rate

ns- # of species in plasma (2 or 3)

The program outputs the particle densities and electric field for the last time step into a data file fdif.res.

```
* PROGRAM FDIF.FOR -- FORTRAN77 -- JOHN LUCAS
* THIS PROGRAM CALCUALTES THE PARTICLE DENSITIES IN A TWO OR
* THREE COMPONENT PLASMA.

      implicit real*8 (a,e,o-z)
      real*8 ne1(10),ne2(10),np1(10),np2(10)
      real*8 e1(0:10),nn1(10),nn2(10),rho(10)
      real*8 v(0:10),kb,k,fe(0:10),fp(0:10)
      real*8 n0,nu,lamda
      integer ts
      real*8 ae(10,10),ani(10,10)
      integer indxn(10),indxe(10)

      open(unit=10,file='fdif.dat',status='old')
      open(unit=11,file='fdif.res',status='old')

      read(10,*)ts
      read(10,*)c
      read(10,*)de
      read(10,*)be
      read(10,*)te,tp
      read(10,*)press
      read(10,*)sigma
      read(10,*)z
      read(10,*)s
      read(10,*)pim
      read(10,*)alpha
      read(10,*)d
      read(10,*)nsp

* Define contstants to be used

      h=1./c
      k=s*h
      kb=1.3807E-23
      em=9.1095E-31
      ec=1.6022E-19
      pi=4.*atan(1.)
      c1=100.*ec/8.8542E-12
      m=int(c)
      n0=press*133.2*6.022E+23/(8.3144*tp*1.0E+06)
      ce1=100.*sqrt(kb*te/(2.*pi*em))
      cp1=100.*sqrt(kb*tp/(2.*pi*pim))
      cp2=100.*sqrt(kb*te/(2.*pi*pim))
      lamda=1./(n0*sigma)
      nu=cp1/lamda
      n=m
      nep=m
      nnp=m

* Call setup to get initial conditions

      call setup(e1,ne1,np1,nn1,nsp)
```

```
* Set up Constant Matrix (Left side) for electrons and
* Negative ion (if present)

      aj1=k*de/h**2
      aj2=(1.-k*(z-alpha)+aj1)
      aj3=(1.-k*(z-alpha)+2.*aj1)

      ae(1,1)=aj2
      ae(1,2)=-aj1
      do 5,jj=2,m-1
       ae(jj,jj-1)=-aj1
       ae(jj,jj)=aj3
       ae(jj,jj+1)=-aj1
00005 continue
      ae(m,m-1)=-aj1
      ae(m,m)=aj2+(k*ce1/h)

* With the constant matrix calculated. Call the sub. LU
* Decomposition to find the decomp. matrix of ae. Decomp.
* Matrix will become the new ae matrix.

      call ludcmp(ae,n,nep,indxe,dae)

* Repeat procedure if negative ions are present

      if (nsp .eq. 3) then
       aj1=((k/h)**2./(1.+k*nu))*(kb*tp/pim)
       aj2=(1.+aj1)
       aj3=(1.+2.*aj1)

       ani(1,1)=aj2
       ani(1,2)=-aj1

       do 7,jj=1,m-1
        ani(jj,jj-1)=-aj1
        ani(jj,jj)=aj3
        ani(jj,jj+1)=-aj1
00007  continue
       ani(m,m-1)=-aj1
       ani(m,m)=aj2+(k/h)*cp1
       call ludcmp(ani,n,nnp,indxn,dn1)
      end if


* Start of time loop

      do 10,j=1,ts

       t2=be*k/(2.*h)
       t3=ne1(1)+ne1(2)
       t1=ne1(1)*(1.+k*d*nn1(1))
       ne2(1)=t1+t2*t3*e1(1)
```

```
      do 15,i=2,m-1
       t1=ne1(i)*(1.+k*d*nn1(i))
       t3=e1(i)*(ne1(i+1)+ne1(i))
       t4=e1(i-1)*(ne1(i)+ne1(i-1))
       ne2(i)=t1+t2*(t3-t4)
00015  continue

       t1=ne1(m)*(1.+k*d*nn1(m))
       t3=e1(m-1)*(ne1(m)+ne1(m-1))
       ne2(m)=t1-t2*t3

       call lubksb(ae,n,nep,indxe,ne2)

00093 continue

* Calculate the ion drift velocities

00107  continue

       v(0)=0.

       vlp=2.*h*lamda/(2.*h+lamda)
       vt2=(ne1(2)+ne1(1))/(np1(2)+np1(1))
       vt3=vlp*vt2*z
       vt4=1.0E+04*ec*e1(1)/pim
       v(1)=.5*(-vt3+sqrt(vt3**2.+4.*vlp*vt4))
       pt1=np1(1)+z*k*ne2(1)
       pt2=(k/h)*v(1)*(np1(1)+np1(2))/2.
       np2(1)=pt1-pt2

       do 20,i=2,m-1
        vt2=(ne1(i+1)+ne1(i))/(np1(i+1)+np1(i))
        vt3=vlp*vt2*z
        vt4=1.0E=04*ec*e1(i)/pim+v(i-1)**2./(2.*h)
        v(i)=.5*(-vt3+sqrt(vt3**2.+4.*vlp*vt4))
        pt1=v(i)*(np1(i+1)+np1(i))
        pt2=v(i-1)*(np1(i-1)+np1(i))
        np2(i)=np1(i)+z*k*ne2(i)-(k/(2.*h)*(pt1-pt2))
00020  continue

       pt1=.5*v(i-1)*(np1(i-1)+np1(m))
       pt2=(k/h)*(np1(m)*cp2-pt1)
       np2(m)=np1(m)+z*k*ne2(m)-pt2
00108  continue

* If negative ions are present setup b matrix

       if (nsp .eq. 3) then
        t1=ec*k**2./(2.*h*pim*(1.+k*nu))
        t2=(1.-k*d*ne1(1))*nn1(1)
        t3=e1(1)*(nn1(1)+nn1(2))
        nn2(1)=t2+k*alpha*ne2(1)+t1*t3
```

```
            do 25,i=2,m-1
             t4=t3
             t2=(1.-k*d*ne1(i))*nn1(i)
             t3=e1(i)*(nn1(i)+nn1(i+1))
             nn2(i)=t2+k*alpha*ne2(i)+t1*(t3-t4)
00025       continue

            t2=(1.-k*d*ne1(m))*nn1(m)
            nn2(m)=t2+k*alpha*ne2(m)-t1*t3

            call lubksb(ani,n,nnp,indxn,nn2)
           end if

* Calculate the Electric field

           e1(0)=0.

           do 30, i=1,m

            rho(i)=np2(i)-ne2(i)-nn2(i)
            e1(i)=e1(i-1)+c1*h*rho(i)

00030      continue

* Set old densities equal to newly calculated densities
* for next time step

           do 35,i=1,m
            ne1(i)=ne2(i)
            np1(i)=np2(i)
            nn1(i)=nn2(i)
00035      continue


00010 continue

           time=k*(j-1)
           write(11,*)'h=',h,'k=',k,'time=',time
           write(11,*)' '
           write(11,*)'Electron Density'
           write(11,200)(ne2(i),ne2(i+1),ne2(i+2),ne2(i+3),ne2(i
+4),
     Xi=1,6,5)
           write(11,*)' '
           write(11,*)'Positive Ion Density'
           write(11,200)(np2(i),np2(i+1),np2(i+2),np2(i+3),np2(i
+4),
     Xi=1,6,5)

           if (nsp .eq. 3) then
            write(11,*)' '
            write(11,*)'Negative Ion Density'
            write(11,200)(nn2(i),nn2(i+1),nn2(i+2),nn2(i+3),nn2(
```

```
i+4),
     Xi=1,6,5)
       end if

       write(11,*)' '
       write(11,*)'Electric Field'
       write(11,200)(e1(i),e1(i+1),e1(i+2),e1(i+3),e1(i+4),
     Xi=0,5,5)
       write(11,300)e1(m)
       write(11,*)' '
       write(11,*)' '

00100  format('
','h=',x,e4.2,x,'k=',x,e6.2,x,'time=',x,e6.2)
00200  format(' ',e11.5,4(2x,e11.5))
00300  format(' ',e11.5)

      end
```

BIBLIOGRAPHY

1. Chen Francis F., Introduction to Plasma Physics, New York: Plenum Press, 1974.

2. Clouse, 2Lt Christopher J. Schottky Theory of Three Component Plasmas, Unpublished MS Thesis GNE/EN/85M-3, School of Engineering, Air Force Institute of Technology (AU), Wright-Patterson AFB OH, January 1985.

3. Edgley, P.D. and A. von Engel. "Theory of positive columns in electronegative gases", Proc. Royal Society London 370: 375-387 (1980).

4. Golant, V.E.,A.P. Zhilinsky and I.E. Sakharov, Fundamentals of Plasma Physics, New York: John Wiley & Sons, 1980.

5. Holt, E.H. and R.E. Haskell Foundations of Plasma Dynamics, New York: Mac Millian Co., 1965.

6. Kline, L. E., "Electron and Chemical Kinetics in the Low-Pressure RF Discharge Etching of Silicon in SF_6", IEEE Transactions on Plasma Science, PS-14 145-150 (April 86).

7. Kushner, Mark J. "Guest Editorial- Special Issue on the Physics of RF Discharges for Plasma Processing", IEEE Transactions on Plasma Science, PS 14 [illegible] April 86.

8. Lee, D. S. and Frank D. Lewis, "Multiple Equilibria in the Oxygen Positive Column", Journal of Applied Physics, [illegible] Sept. 1980.

9. McDaniel, Earl W. Collisional Phenomena in Ionized Gases, New York: Wiley and Sons, 1964.

10. Press, William H., et al. Numerical Recipes, The Art of Scientific Computing, Cambridge: Cambridge University Press, 1986.

11. Rockwood, Stephen D., "Elastic and Inelastic Cross Sections for Electron-Hg Scattering for Hg Transport Data", Physical Review A, Vol 8, No. 5, 2348-2358 (November 1973).

12. Rogoff, Geranld L. et al. "A Model for thr Buld Plasma in an RF Chlorine Discharge, "IEE Transactions on Plasma Science, PS-14: 103-110 (April 86).

13 Reif, F. Fundamentals of Statistical and Thermal Physics, New York: McGraw Hill, 1965.

14. Self, S.A. and H.N. Ewald "Static Theory of a Discharge Column at Intermediate Pressures", The Physics of Fluids, Vol 9, number 12, 2486-2492, December 1966.

15. Tsendin, L.D. "Diffusion of Charged Particles in Plasmas of Electronegative Gases", Soviet Technical Physics, 30: 1377-1379, December 1985.

16. Wunderer, B. M. "Ambipolar Diffusion in a Nonuniform Plasma Containing Positive Ion Component", IEEE Transactions on Plasma Science, Vol PS-6: 406-415 (December 1978).

VITA

John C. Lucas was born on 8 August 1961 in Marion, Illinois. He graduated from high school in Marion, Illinois, in 1979 and attended Southern Illinois University-Carbondale from which he received the degree of Bachelor of Science in Physics. Upon graduation in May 83, he received a commission in the USAF through the ROTC program. In September 1983, he was called to active duty. He worked as a acquisition project officer on the C-21A/C-12F program from September 83 until entering AFIT in August 1985.

Permanent address: 1205 E. Carter St.
Marion, IL 62959

UNCLASSIFIED
SECURITY CLASSIFICATION OF THIS PAGE

AD-A176 919

REPORT DOCUMENTATION PAGE

Form Approved OMB No. 0704-0188

1a. REPORT SECURITY CLASSIFICATION: UNCLASSIFIED	1b. RESTRICTIVE MARKINGS
2a. SECURITY CLASSIFICATION AUTHORITY	3. DISTRIBUTION/AVAILABILITY OF REPORT: Approved for Public release; distribution unlimited.
2b. DECLASSIFICATION/DOWNGRADING SCHEDULE	
4. PERFORMING ORGANIZATION REPORT NUMBER(S): AFIT/GNE-87M-4	5. MONITORING ORGANIZATION REPORT NUMBER(S)
6a. NAME OF PERFORMING ORGANIZATION: School of Engineering Air Force of Technology; 6b. OFFICE SYMBOL (If applicable): AFIT/ENP	7a. NAME OF MONITORING ORGANIZATION
6c. ADDRESS (City, State, and ZIP Code): Wright-Patterson AFB, OH 45433	7b. ADDRESS (City, State, and ZIP Code)
8a. NAME OF FUNDING/SPONSORING ORGANIZATION; 8b. OFFICE SYMBOL (If applicable)	9. PROCUREMENT INSTRUMENT IDENTIFICATION NUMBER
8c. ADDRESS (City, State, and ZIP Code)	10. SOURCE OF FUNDING NUMBERS: PROGRAM ELEMENT NO; PROJECT NO; TASK NO; WORK UNIT ACCESSION NO

11. TITLE (Include Security Classification)
DEVELOPMENT OF A GENERALIZED MODEL FOR A THREE COMPONENT PLASMA (UNCLASSIFIED)

12. PERSONAL AUTHOR(S)
Lucas, B John , C.

13a. TYPE OF REPORT	13b. TIME COVERED	14. DATE OF REPORT (Year, Month, Day)	15. PAGE COUNT
MS THESIS	FROM _____ TO _____	1987 JAN	89

16. SUPPLEMENTARY NOTATION

17. COSATI CODES			18. SUBJECT TERMS (Continue on reverse if necessary and identify by block number)
FIELD	GROUP	SUB-GROUP	
20	09		Plasmas, Electronegative Plasmas, Plasma Diffusion

19. ABSTRACT (Continue on reverse if necessary and identify by block number)

Thesis Chairman: Dr. William Bailey
Professor of Physics

Approved for public release: LAW AFR 190-1.
LYNN E. WOLAVER
Dean for Research and Professional Development
Air Force Institute of Technology
Wright-Patterson AFB OH 45433
April 87

20. DISTRIBUTION/AVAILABILITY OF ABSTRACT	21. ABSTRACT SECURITY CLASSIFICATION
☒ UNCLASSIFIED/UNLIMITED ☐ SAME AS RPT ☐ DTIC USERS	Unclassified
22a. NAME OF RESPONSIBLE INDIVIDUAL: Dr. William Bailey	22b. TELEPHONE (Include Area Code): (513)-255-2012; 22c. OFFICE SYMBOL: AFIT/ENP

DD Form 1473, JUN 86 — Previous editions are obsolete

SECURITY CLASSIFICATION OF THIS PAGE
UNCLASSIFIED

The purpose of this ~~study is to~~ thesis develops a generalized model of a three component plasma which prdicts the density profiles of the charged particles. The plasma was modeled using a finite difference solution to the charged particle continuity and momentum equations. The plasma-sheath boundary is treated by applying the Bohm criterion.

The code developed was sucessful in modeling one component diffusion. However attempts to apply the model to two component plasmas resulted in numerical instabilities and therefore prevented application of the model to a three component plasma.

END

5-87

DTIC